Measurements of two-particle azimuthal and pseudorapidity correlations from ATLAS

Sooraj Radhakrishnan
(*on behalf of the ATLAS collaboration*)

p+Pb azimuthal correlations: *Phys. Rev. C* ***90****, 044906 (2014)*
Pb+Pb pseudorapidity correlations: *ATLAS-CONF-2015-020*

Measurement of two-particle pseudorapidity correlation in Pb+Pb collisions at $\sqrt{s_{NN}} = 2.76$ TeV with ATLAS detector

Sooraj Radhakrishnan
(*on behalf of the ATLAS collaboration*)

Pb+Pb pseudorapidity correlations: *ATLAS-CONF-2015-020*

Introduction

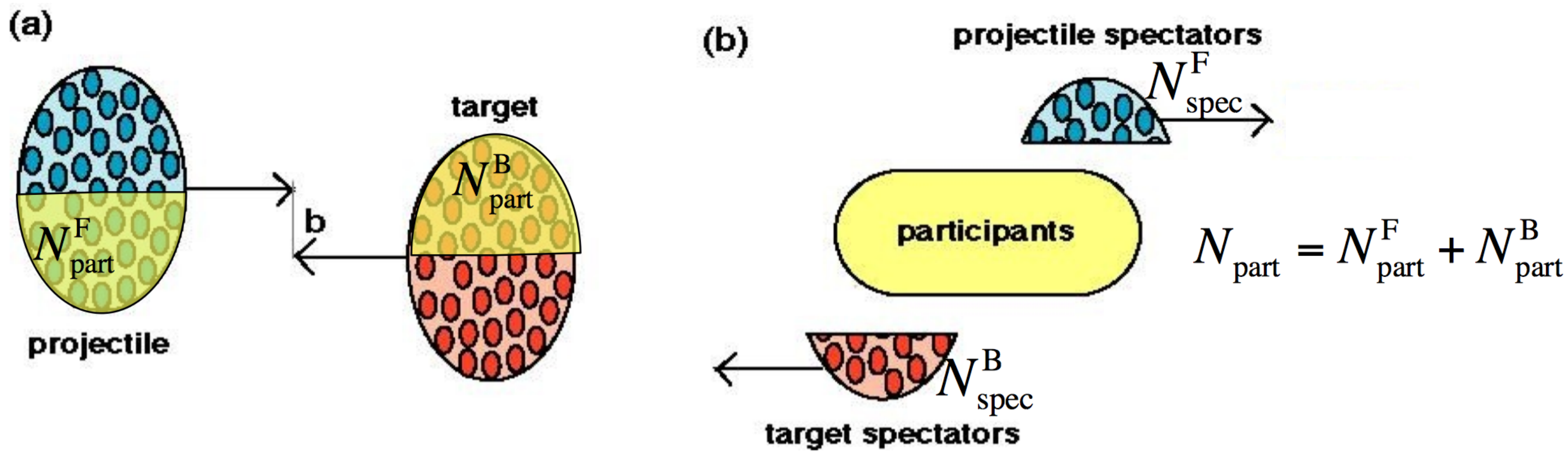

- One of the largest uncertainties in the modeling of heavy-ion collision arises from present poor understanding of the early-time dynamics especially in the longitudinal direction.

- Event-by-event, A-A collisions are not symmetric and are not boost invariant systems.
  - eg: $N^{F}_{part} \neq N^{B}_{part}$, produces asymmetry in the final distribution

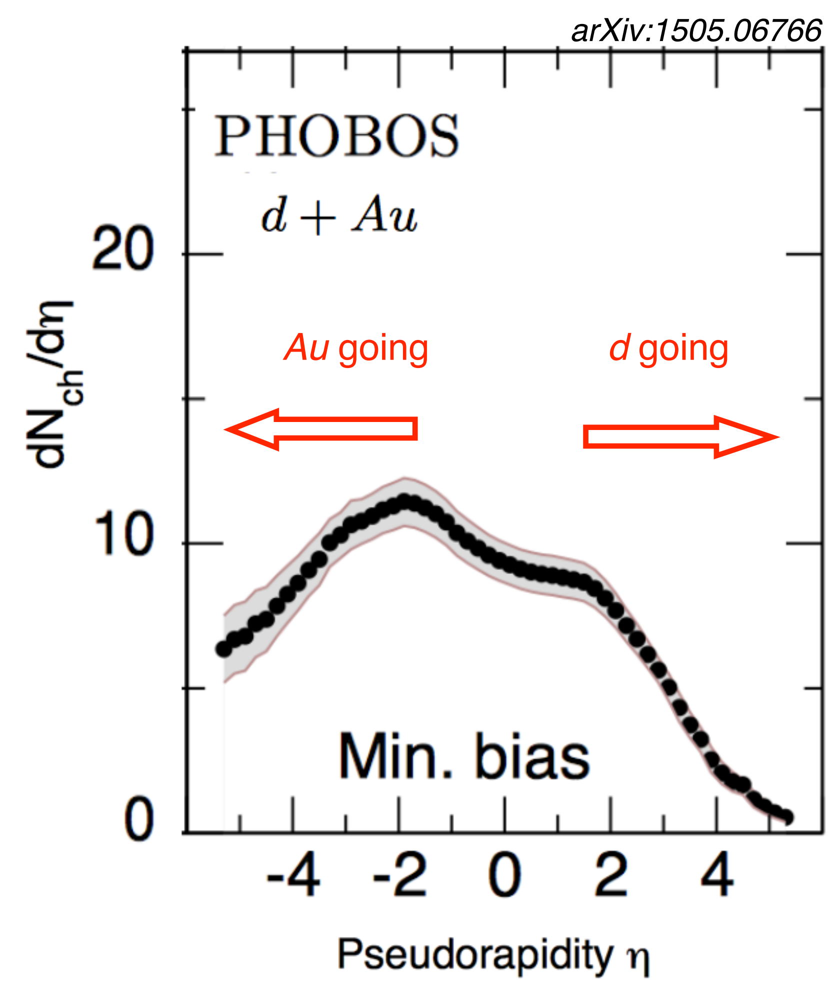

- Longitudinal correlations can probe rapidity profile of the initial fireball density.
- Also, charge correlations, medium effects, ..

- Rich and interesting physics, but under explored!

Introduction

- A simple wounded nucleon model predicts large event-by-event linear fluctuation in multiplicity, assuming a linear emission profile in rapidity for each wounded nucleon *(A.Bzdak,D.Teaney: 1210.1965)*
- But there can also be higher-order fluctuations.

Asymmetry in initial state

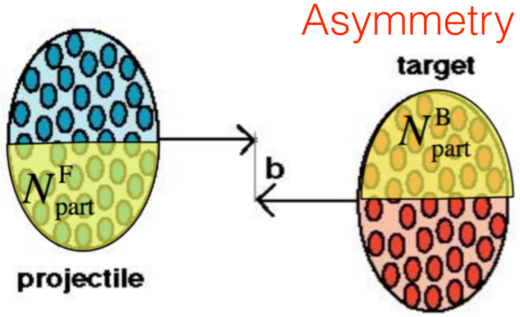

$$A_{N_{\rm part}} = \frac{N^{\rm F}_{\rm part} - N^{\rm B}_{\rm part}}{N^{\rm F}_{\rm part} + N^{\rm B}_{\rm part}}\,.$$

Asymmetry in final state

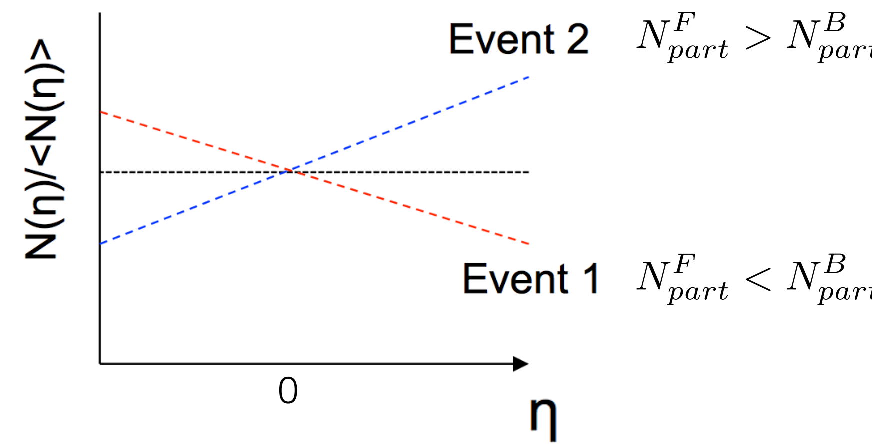

- Previous measurements focused on forward-backward asymmetry, eg: correlation coefficient between two symmetric rapidity windows.

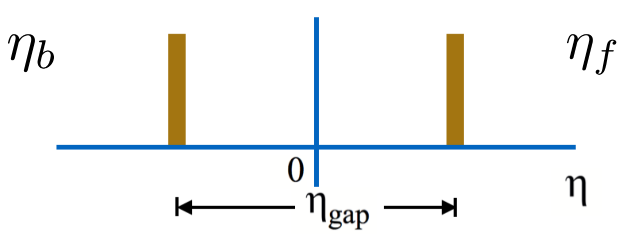

$$b = \frac{\langle N_f N_b\rangle - \langle N_f\rangle\langle N_b\rangle}{\langle N_f^2\rangle - \langle N_f\rangle^2}$$

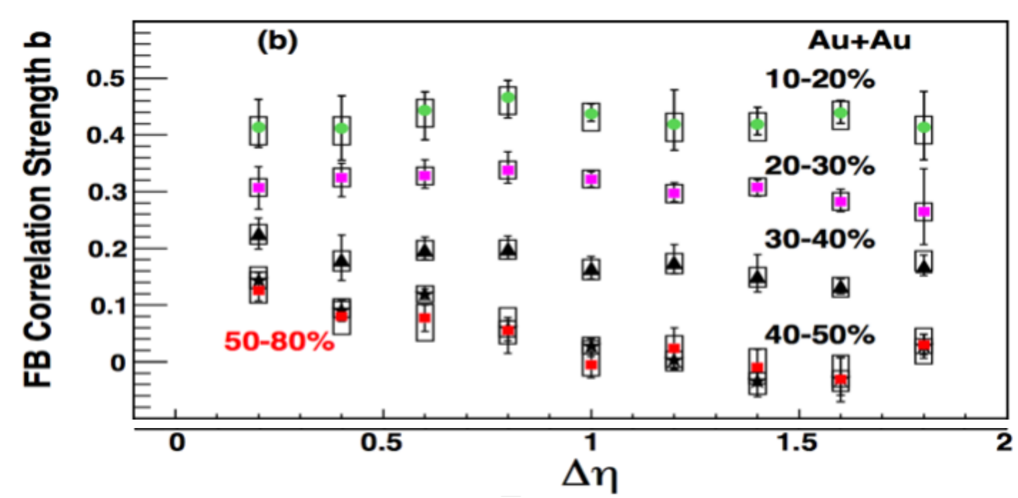

STAR
Phys.Rev.Lett. 103:172301,2009

- Biased by statistics in the bins, also not the full correlation map.
- New proposals: measure correlation function in η_1, η_2 *(1210.1965, 1506.03496, see poster by M.Zhou)*

Quantifying shape fluctuations

- Event-by-event shape fluctuations may be expanded in an ortho-normal set of polynomials, eg: Legendre polynomials

$$N(\eta) = \langle N(\eta) \rangle \left(1 + \sum_{n=0}^{\infty} a_n T_n(\eta) \right), \quad T_n(\eta) = \sqrt{n + \frac{1}{2}} P_n(\eta / Y)$$

$$P_0(x) = 1, \quad P_1(x) = x, \quad P_2(x) = \frac{1}{2}(3x^2 - 1) \;, \ldots.$$

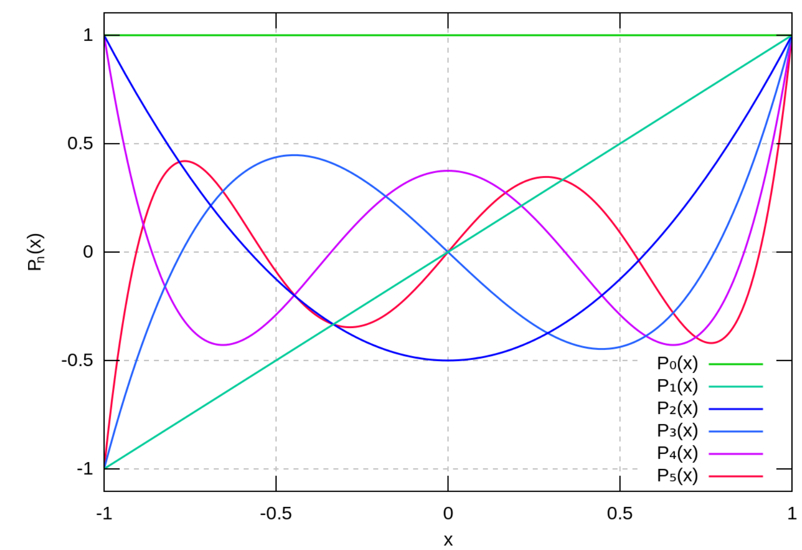

First few Legendre Polynomials

- a_0 quantifies overall multiplicity fluctuations,
- a_1 quantifies the linear component of the FB asymmetry of $N(\eta)$,
- a_2 quantifies difference in $N(\eta)$ between mid and forward rapidities (from different amounts of nuclear stopping(?)),
- …
- In this analysis, interested in a_1, a_2 and higher order terms which quantify shape fluctuations

Quantifying shape fluctuations

- Event-by-event shape fluctuations may be expanded in an ortho-normal set of polynomials, eg: Legendre polynomials

$$N(\eta) = \langle N(\eta)\rangle \left(1 + \sum_{n=0}^{\infty} a_n T_n(\eta)\right), \quad T_n(\eta) = \sqrt{n+\frac{1}{2}}P_n(\eta/Y)$$

$$P_0(x) = 1, \quad P_1(x) = x, \quad P_2(x) = \frac{1}{2}(3x^2-1)\,, \ldots .$$

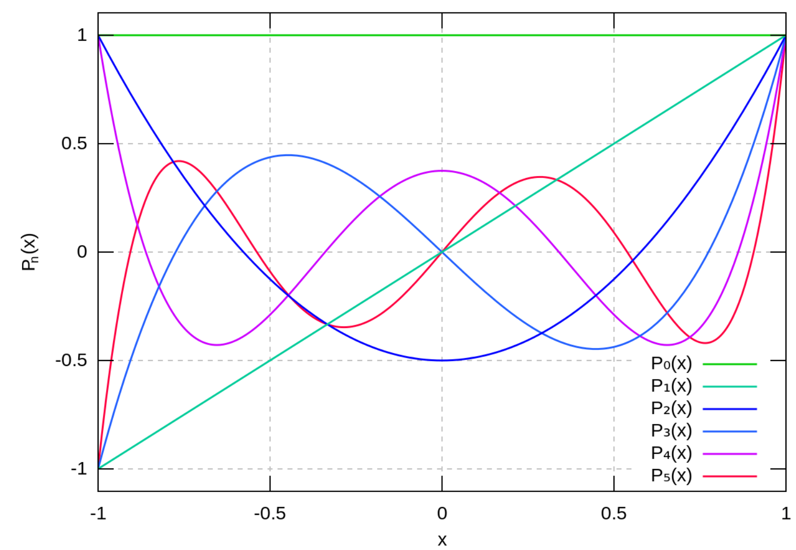

First few Legendre Polynomials

- Define the two particle correlation function: $C(\eta_1,\eta_2) = \dfrac{\langle N(\eta_1)N(\eta_2)\rangle}{\langle N(\eta_1)\rangle\langle N(\eta_2)\rangle}$

- If $\langle a_n\rangle = 0$, the correlation function can be used to extract the r.m.s and correlations of the e-b-e modulations

$$C(\eta_1,\eta_2) = 1 + \sum_{n=0}^{\infty}\langle a_n a_m\rangle\left(\frac{T_n(\eta_1)T_m(\eta_2)+T_n(\eta_2)T_m(\eta_1)}{2}\right)$$

==> $\langle a_n a_m\rangle$ can be obtained from a discrete transform of CF into the chosen basis.

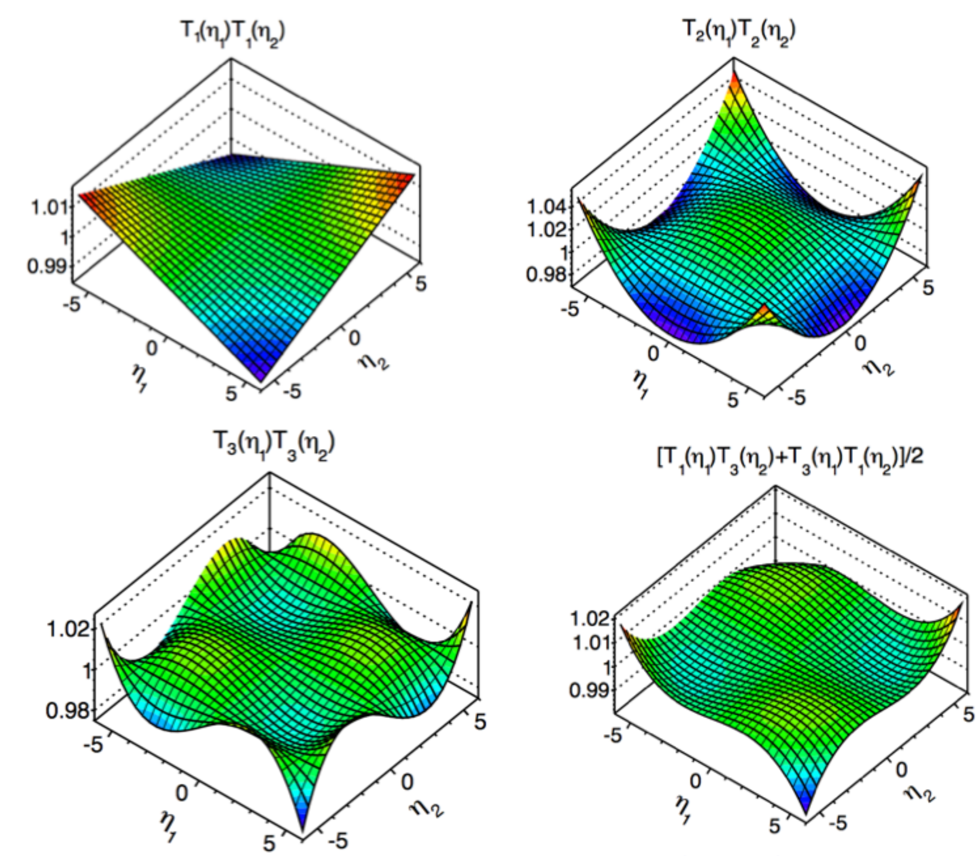

Shape of base functions in 2D with $\langle a_n a_m\rangle = 0.01$

Analysis procedure

- Analysis using 2.76 TeV Pb+Pb collisions at LHC recorded by the ATLAS detector

- Correlation functions constructed from charged particle tracks reconstructed in ATLAS Inner Detector in $|\eta| < 2.4$ and having $p_{\mathrm{T}} >$ 0.5 GeV

$$C(\eta_1, \eta_2) = \frac{\langle N(\eta_1) N(\eta_2) \rangle}{\langle N(\eta_1) \rangle \langle N(\eta_2) \rangle}$$

$$= \frac{\langle N^{same}_{pairs}(\eta_1, \eta_2) \rangle}{\langle N^{mix}_{pairs}(\eta_1, \eta_2) \rangle}$$

- Events for mixing chosen to have similar multiplicity and detector conditions as the foreground event.

- Robust procedure to minimize detector effects
- Not biased by statistics in the bins.

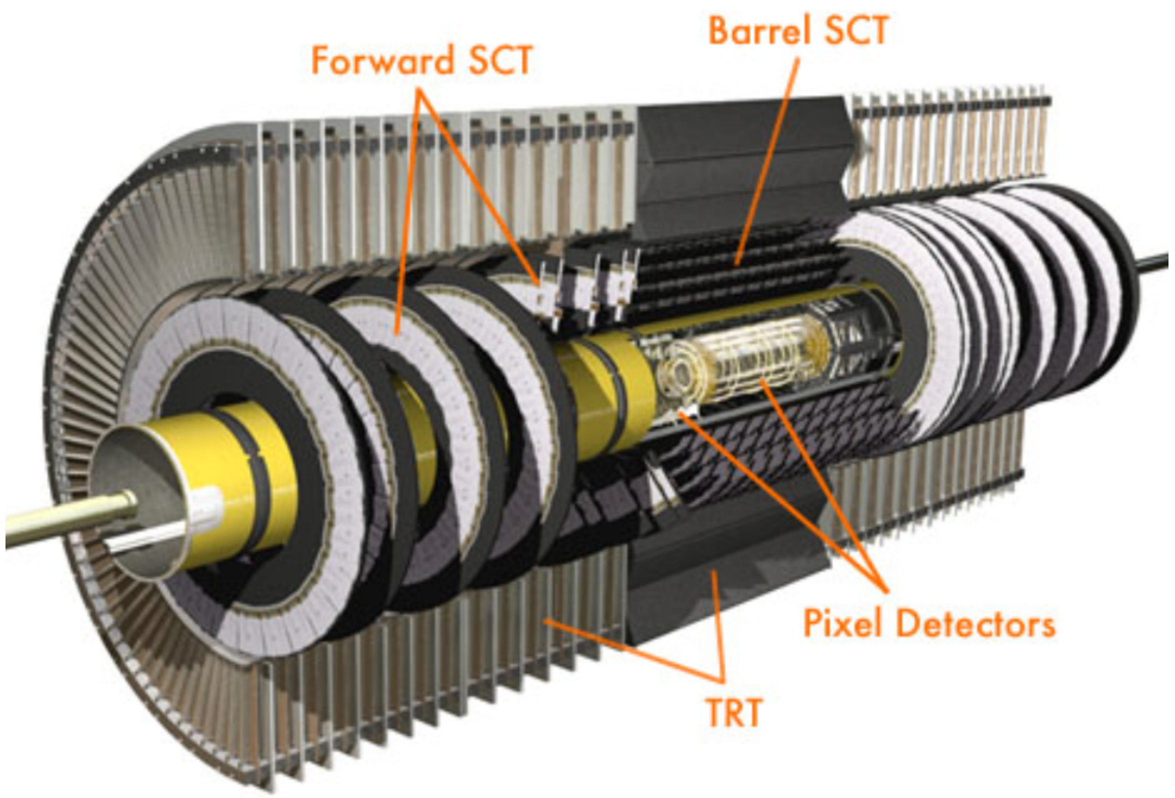

ATLAS Inner Detector System

Analysis procedure: Residual centrality dependence

- Apply a rescaling by the projections to remove residual centrality dependence

$$\boxed{C_N(\eta_1,\eta_2) = \frac{C(\eta_1,\eta_2)}{C_p(\eta_1)C_p(\eta_2)} \qquad C_p(\eta_1) = \int \frac{C(\eta_1,\eta_2)}{2Y}d\eta_2, C_p(\eta_2) = \int \frac{C(\eta_1,\eta_2)}{2Y}d\eta_1; Y = 2.4}$$

- Removes contributions from shape changes correlated with change in multiplicity, does not affect higher order terms ($\langle a_n a_m \rangle$ with n,m > 0)

$$C(\eta_1,\eta_2) = 1 + \boxed{\langle a_0 a_0 \rangle + \sum_{n=1}^{\infty} \langle a_0 a_n \rangle \left(T_n(\eta_2) + T_n(\eta_1)\right)} + \sum_{n,m=1}^{\infty} \langle a_n a_m \rangle \frac{\left(T_n(\eta_1)T_m(\eta_2) + T_n(\eta_2)T_m(\eta_1)\right)}{2}$$

$$C_N(\eta_1,\eta_2) = 1 + \sum_{n=1}^{\infty} \langle a_n a_m \rangle \left(\frac{T_n(\eta_1)T_m(\eta_2) + T_n(\eta_2)T_m(\eta_1)}{2}\right)$$

Analysis procedure: Residual centrality dependence

for more detais see arXiv:1506.03496

- Apply a rescaling by the projections to remove residual centrality dependence

$$\boxed{C_N(\eta_1,\eta_2) = \frac{C(\eta_1,\eta_2)}{C_p(\eta_1)C_p(\eta_2)} \qquad C_p(\eta_1) = \int \frac{C(\eta_1,\eta_2)}{2Y}d\eta_2, C_p(\eta_2) = \int \frac{C(\eta_1,\eta_2)}{2Y}d\eta_1; Y = 2.4}$$

- Removes contributions from shape changes correlated with change in multiplicity, does not affect higher order terms ($\langle a_n a_m \rangle$ with n,m > 0)

$$C(\eta_1,\eta_2) = 1 + \boxed{\langle a_0 a_0 \rangle + \sum_{n=1}^{\infty} \langle a_0 a_n \rangle \left(T_n(\eta_2) + T_n(\eta_1)\right)} + \sum_{n,m=1}^{\infty} \langle a_n a_m \rangle \frac{(T_n(\eta_1)T_m(\eta_2) + T_n(\eta_2)T_m(\eta_1))}{2}$$

$$C_N(\eta_1,\eta_2) = 1 + \sum_{n=1}^{\infty} \langle a_n a_m \rangle \left(\frac{T_n(\eta_1)T_m(\eta_2) + T_n(\eta_2)T_m(\eta_1)}{2}\right)$$

$\boxed{C(\eta_1,\eta_2)}$

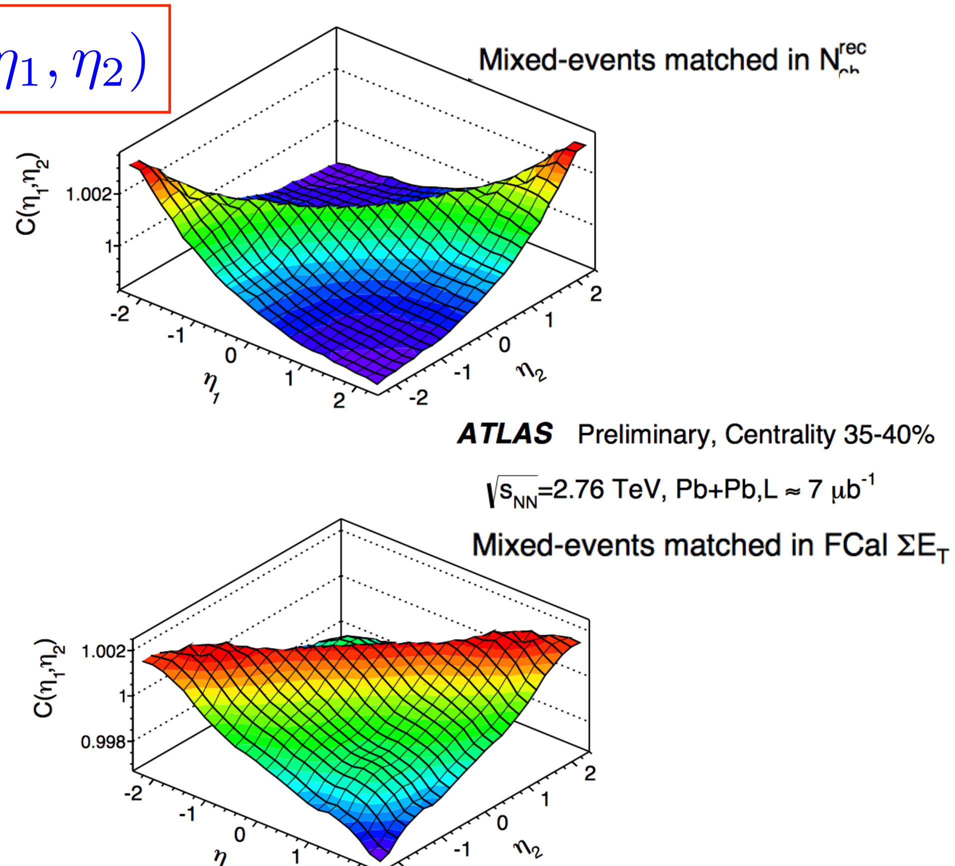

$\boxed{C_N(\eta_1,\eta_2)}$

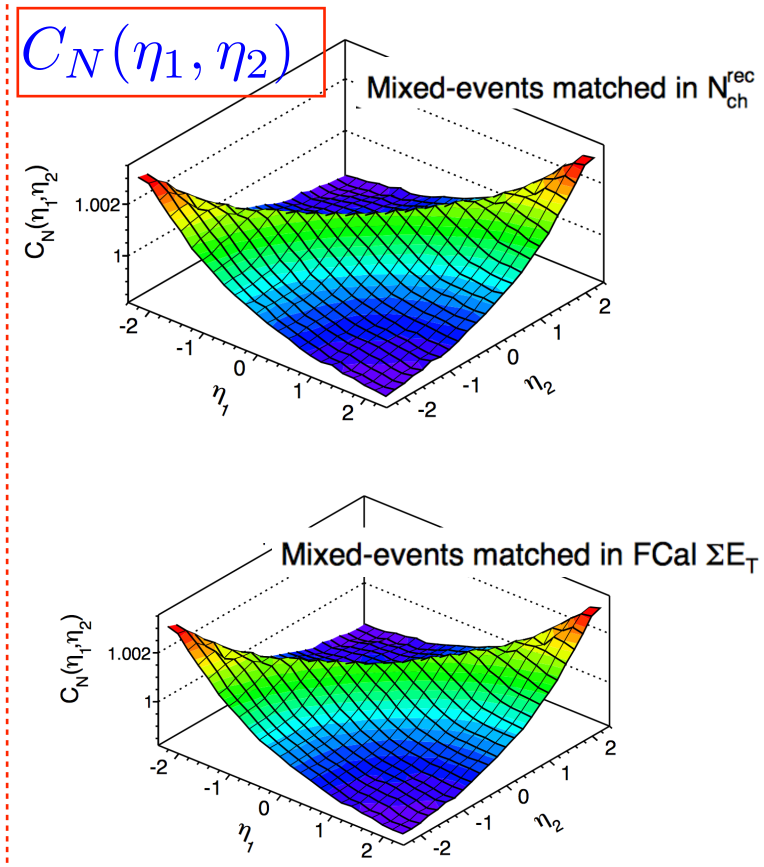

- $\langle a_0 a_n \rangle$ causes CF to look different depending on the multiplicity bin widths used for single particle averages

$$C(\eta_1,\eta_2) = \frac{\langle N(\eta_1)N(\eta_2)\rangle}{\langle N(\eta_1)\rangle\langle N(\eta_2)\rangle}$$

- After rescaling by projections consistent for different bin widths

Results: Correlation Functions

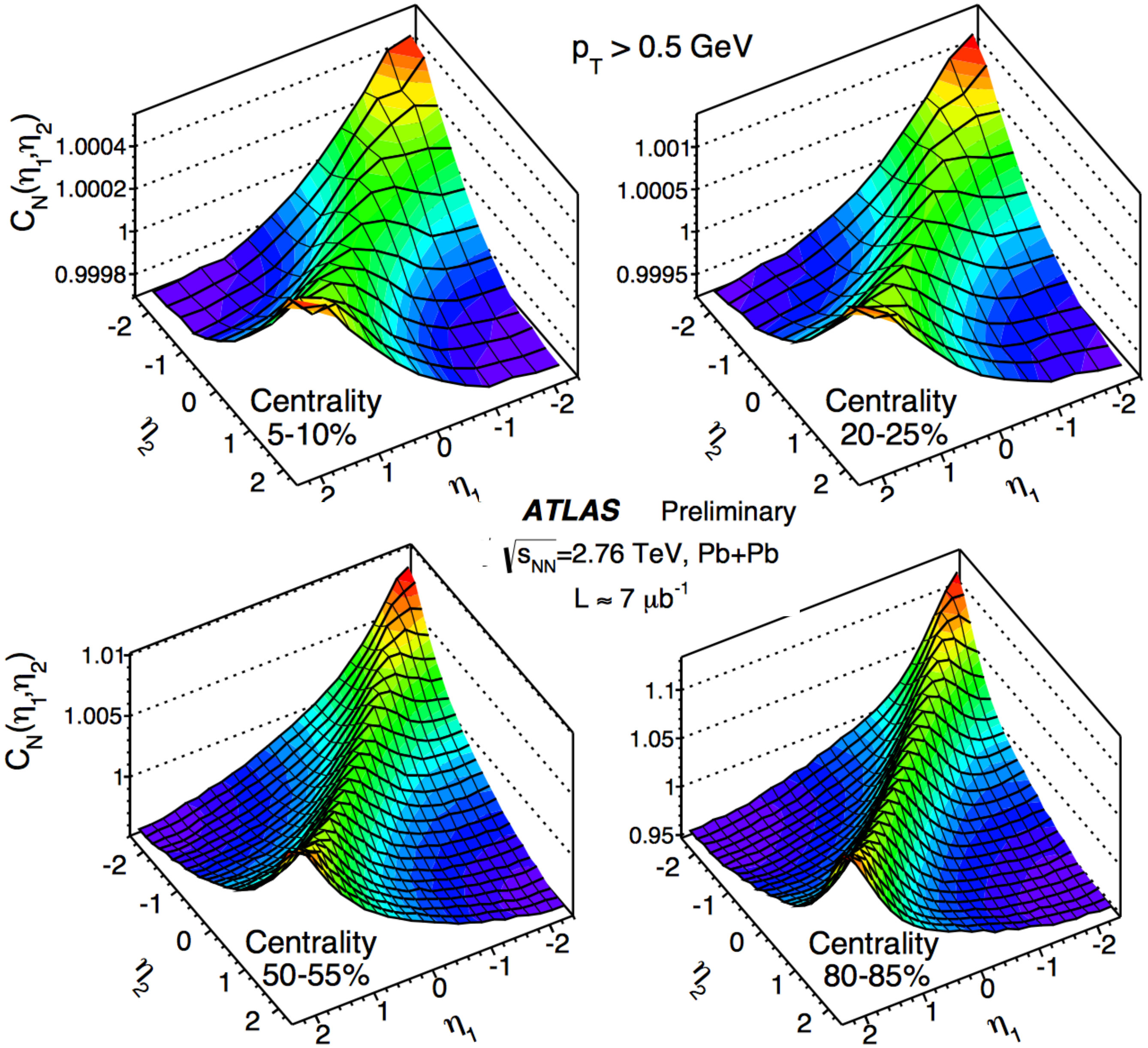

- Correlation signal increases with centrality, expected, as the participant asymmetry A_{Npart} grows with centrality
- Ridge along diagonal narrows towards peripheral —> Increase in short range correlations

$$A_{N_{\text{part}}} = \frac{N^{\text{F}}_{\text{part}} - N^{\text{B}}_{\text{part}}}{N^{\text{F}}_{\text{part}} + N^{\text{B}}_{\text{part}}}.$$

Results: Correlation Functions

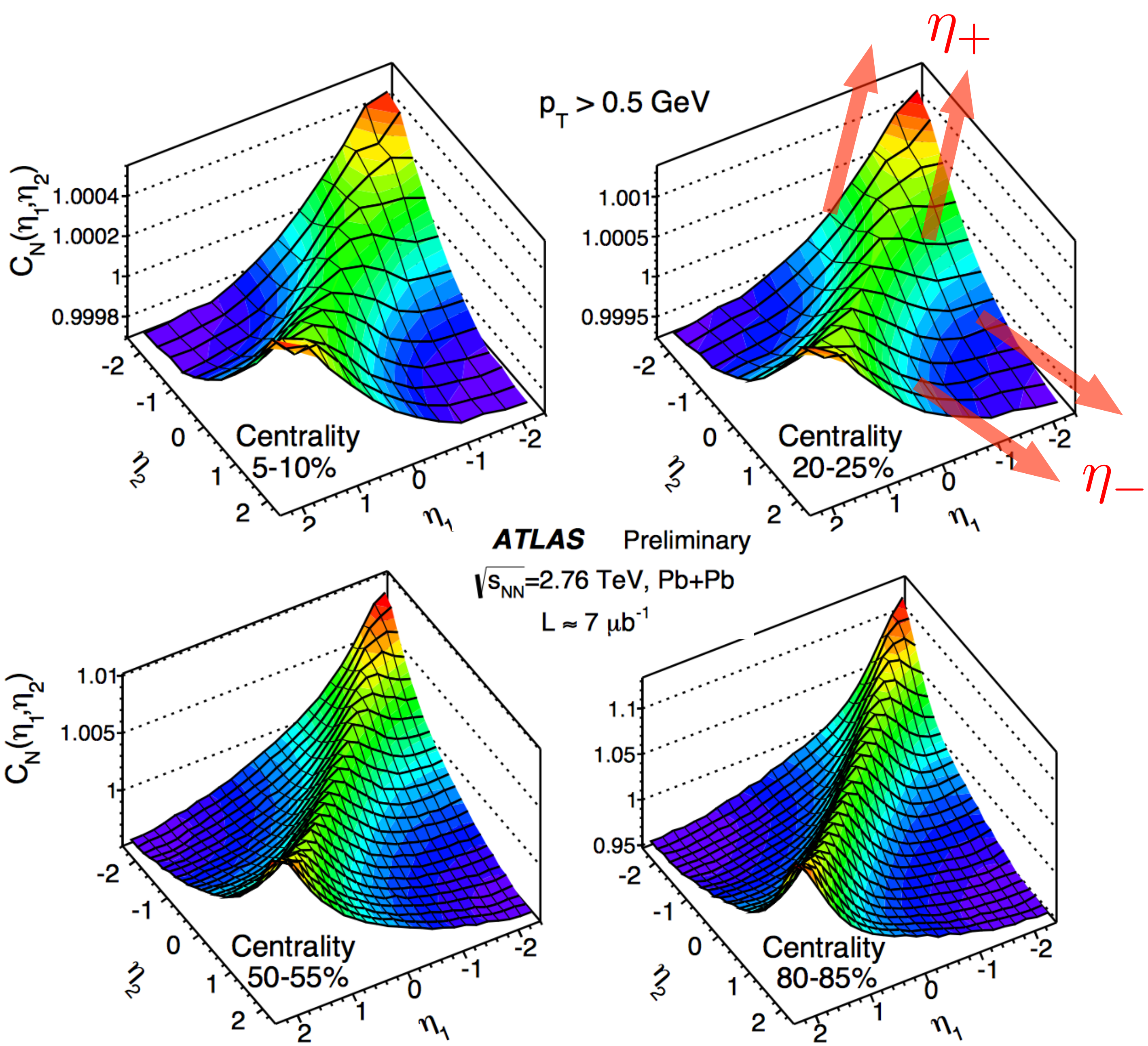

- If the first order (linear) modulation is dominating event-by-event, then,

$$C_N(\eta_1,\eta_2) \sim 1 + \langle a_1^2 \rangle \frac{3}{2Y^2}\eta_1\eta_2$$

- In terms of $\eta_+ = \eta_1 + \eta_2$ and $\eta_- = \eta_1 - \eta_2$,

$$C_N(\eta_-,\eta_+) \sim 1 + \langle a_1^2 \rangle \frac{3}{8Y^2}(\eta_+^2 - \eta_-^2)$$

$$\approx 1 + 0.065\langle a_1^2 \rangle (\eta_+^2 - \eta_-^2)$$

- Correlation function should be dominated by the quadratic dependence along η_+ and η_-

$$C_N(\eta_1,\eta_2) = 1 + \sum_{n=1}^{\infty} \langle a_n a_m \rangle \left(\frac{T_n(\eta_1)T_m(\eta_2) + T_n(\eta_2)T_m(\eta_1)}{2} \right)$$

$$T_1(\eta) = \sqrt{\frac{3}{2}}\frac{\eta}{Y} , \quad Y = 2.4$$

Results: Projections of CF

Projections along η_- :

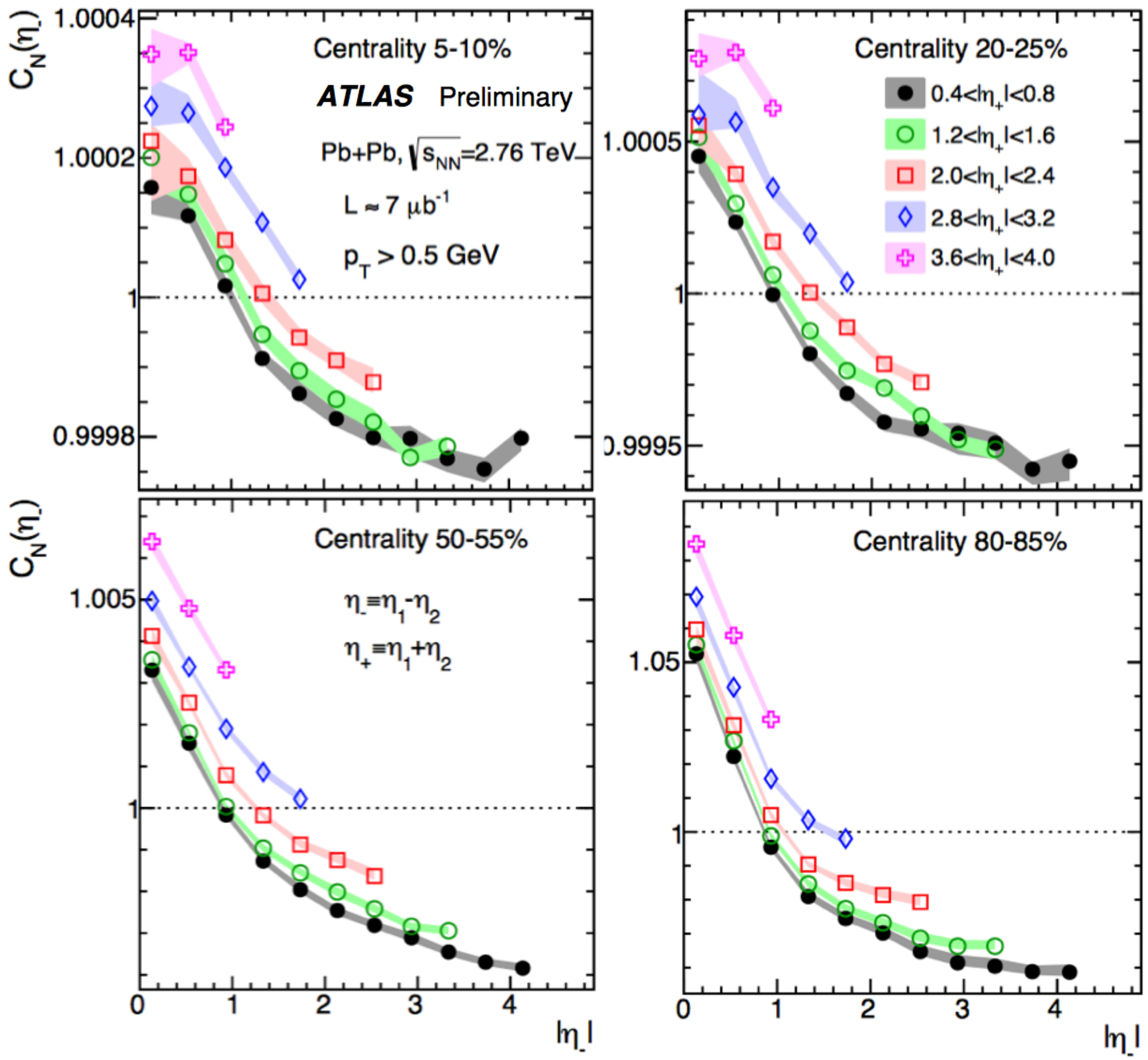

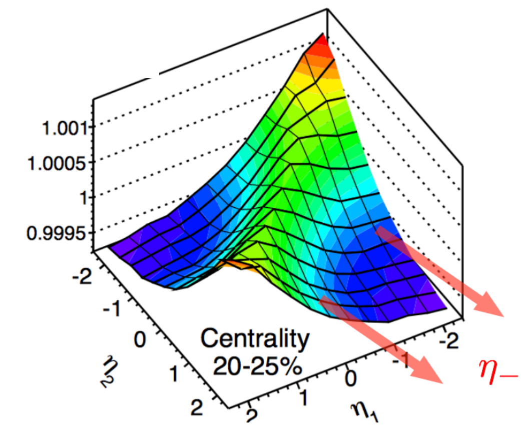

$$\eta_- = \eta_1 - \eta_2$$

- Correlation strength drops fast for $|\eta_-|<1$, decreases more slowly beyond
- Quadratic dependence not clear,
- Short-range correlations also have strong dependence on η_-

- Previous measurements also were concerned with η_- dependence, but only at $\eta_+ = 0$.

$$C_N(\eta_-,\eta_+) \sim 1 + \langle a_1^2\rangle \frac{3}{8Y^2}(\eta_+^2 - \eta_-^2) \quad \approx 1 + 0.065\langle a_1^2\rangle(\eta_+^2 - \eta_-^2)$$

Results: Projections of CF

Projections along η_+ :

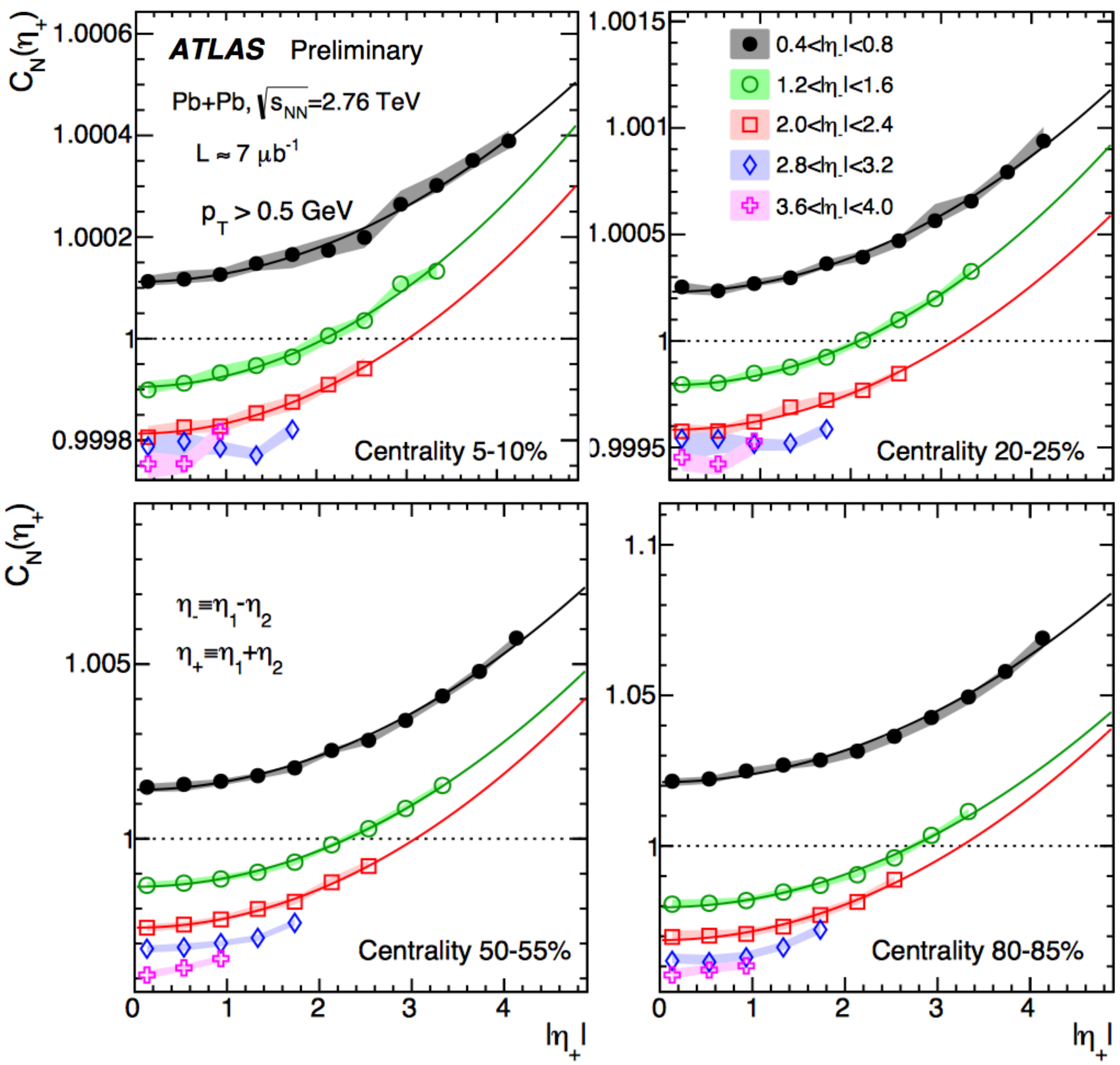

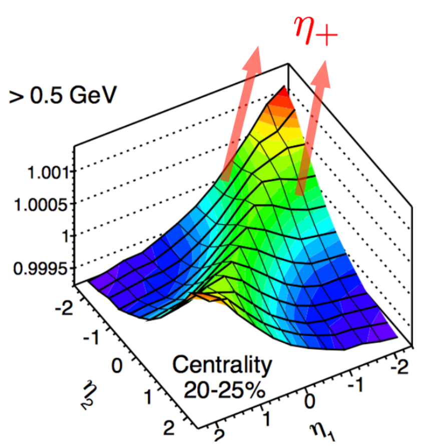

$$\eta_+ = \eta_1 + \eta_2$$

- Solid lines are fits to $$C_N(\eta_+) = 0.065\langle a_1^2\rangle \eta_+^2 + b$$

- Quadratic dependence for all η_- .
- Short-range correlations mainly change the pedestal 'b'.

- Could help disentangle short-range and long-range correlations.

$$C_N(\eta_-, \eta_+) \sim 1 + \langle a_1^2\rangle \frac{3}{8Y^2}(\eta_+^2 - \eta_-^2) \quad \approx 1 + 0.065\langle a_1^2\rangle(\eta_+^2 - \eta_-^2)$$

Results: Linear component from fit

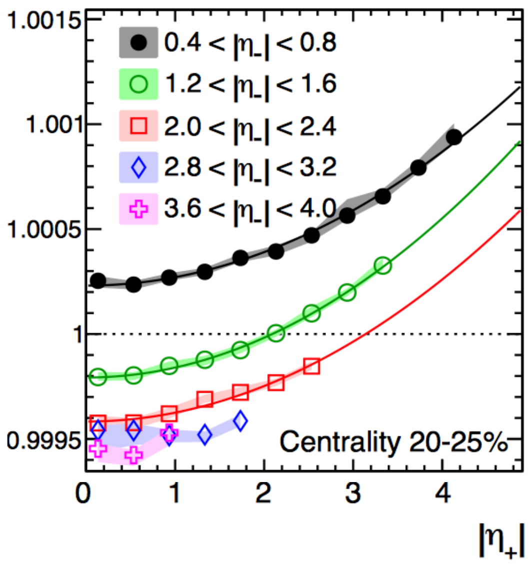

$$C_N(\eta_+) = 0.065\boxed{\langle a_1^2 \rangle}\eta_+^2 + b$$

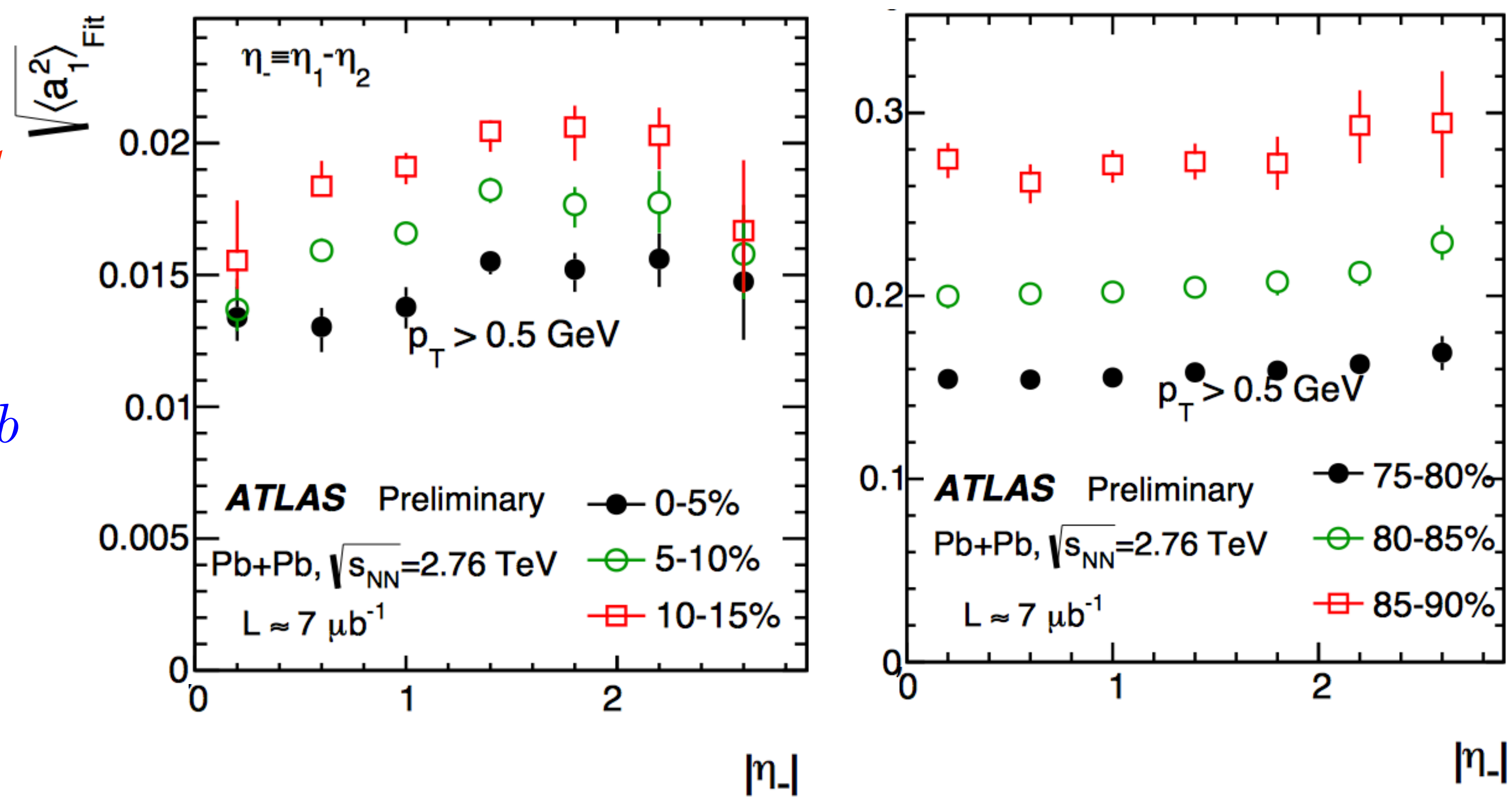

- $\sqrt{\langle a_1^2 \rangle}_{\mathrm{Fit}}$ from fit to projections along η_+ from different η_- slices.
- $\sqrt{\langle a_1^2 \rangle}_{\mathrm{Fit}}$ grows rapidly with centrality.
- Weak dependence on η_-, the fit values are not very sensitive to short-range correlations.

Results: Legendre coefficients, spectra

$$C_N(\eta_1, \eta_2) = 1 + \sum_{n=1}^{\infty} \langle a_n a_m \rangle \left(\frac{T_n(\eta_1)T_m(\eta_2) + T_n(\eta_2)T_m(\eta_1)}{2} \right)$$

Results: Legendre coefficients, spectra

$$C_N(\eta_1,\eta_2) = 1 + \sum_{n=1}^{\infty} \langle a_n a_m \rangle \left(\frac{T_n(\eta_1)T_m(\eta_2) + T_n(\eta_2)T_m(\eta_1)}{2} \right)$$

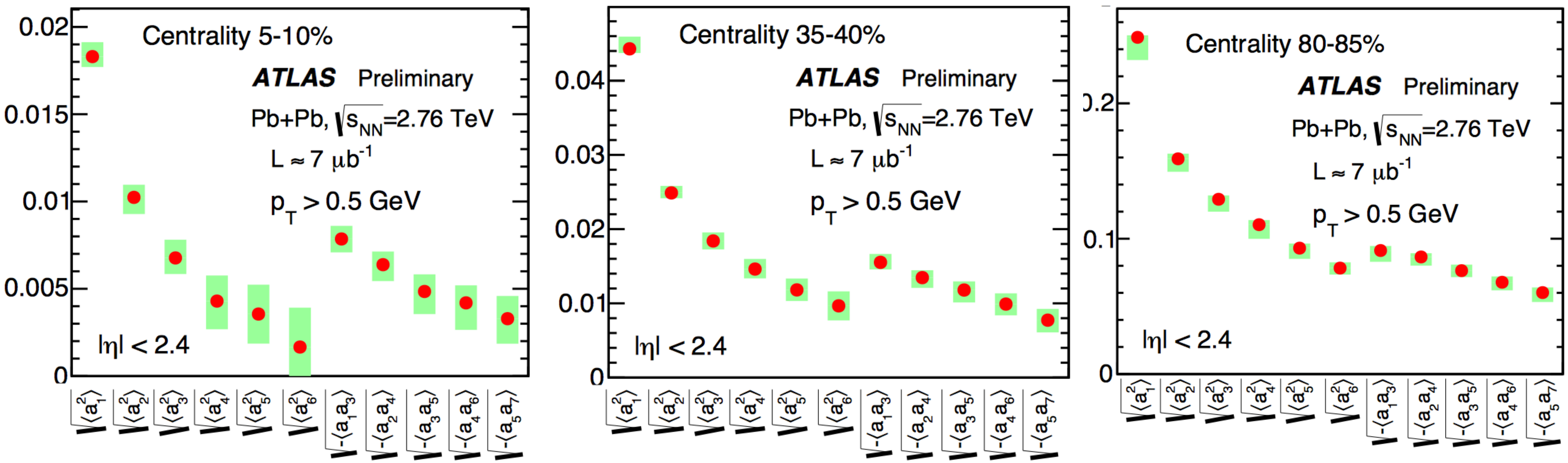

$\sqrt{\langle a_n^2 \rangle}$ for n = 1,..,6 and $\sqrt{-\langle a_n a_{n+2} \rangle}$ for n = 1,..,5

- Linear modulation, $\sqrt{\langle a_1^2 \rangle}$ is the largest, but there are higher order modes with non-zero values. Non-zero values observed for $\sqrt{\langle a_n^2 \rangle}$ and $\sqrt{-\langle a_n a_{n+2} \rangle}$
- The magnitude of the coefficients decrease with n.
- In most central classes coefficients drop to zero for large n, but in peripheral classes they stay non-zero, could be from increased short-range correlations.

Results: Legendre coefficients, centrality dependence

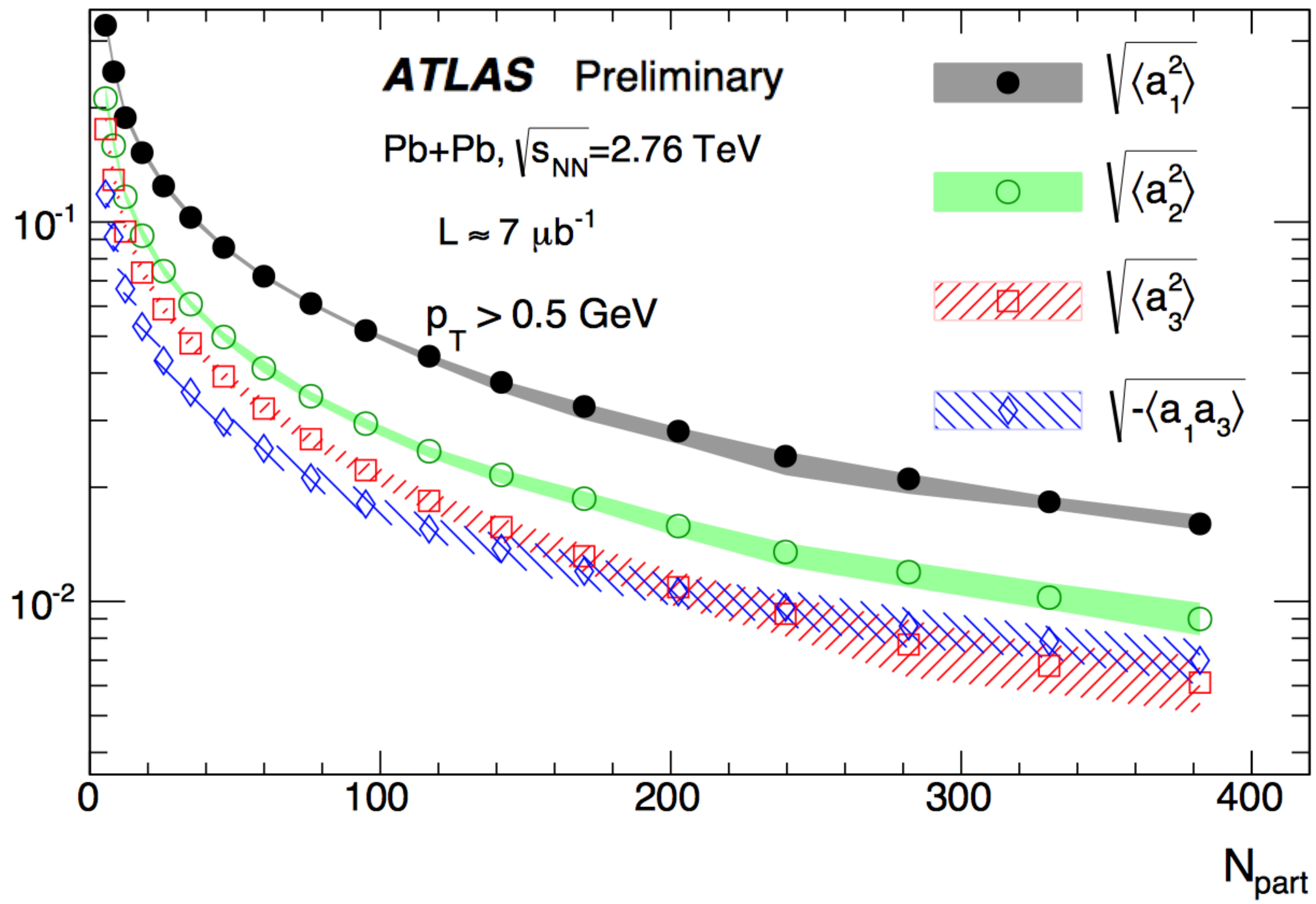

- $\sqrt{a_1^2}, \sqrt{a_2^2}, \sqrt{a_3^2}, \sqrt{-a_1 a_3}$ as a function of N_{part}
- Values are small in central collisions, but grow to more than 10% in peripheral collisions.
- Similar N_{part} dependence for the leading coefficients.

Results: Comparison to values from Fit

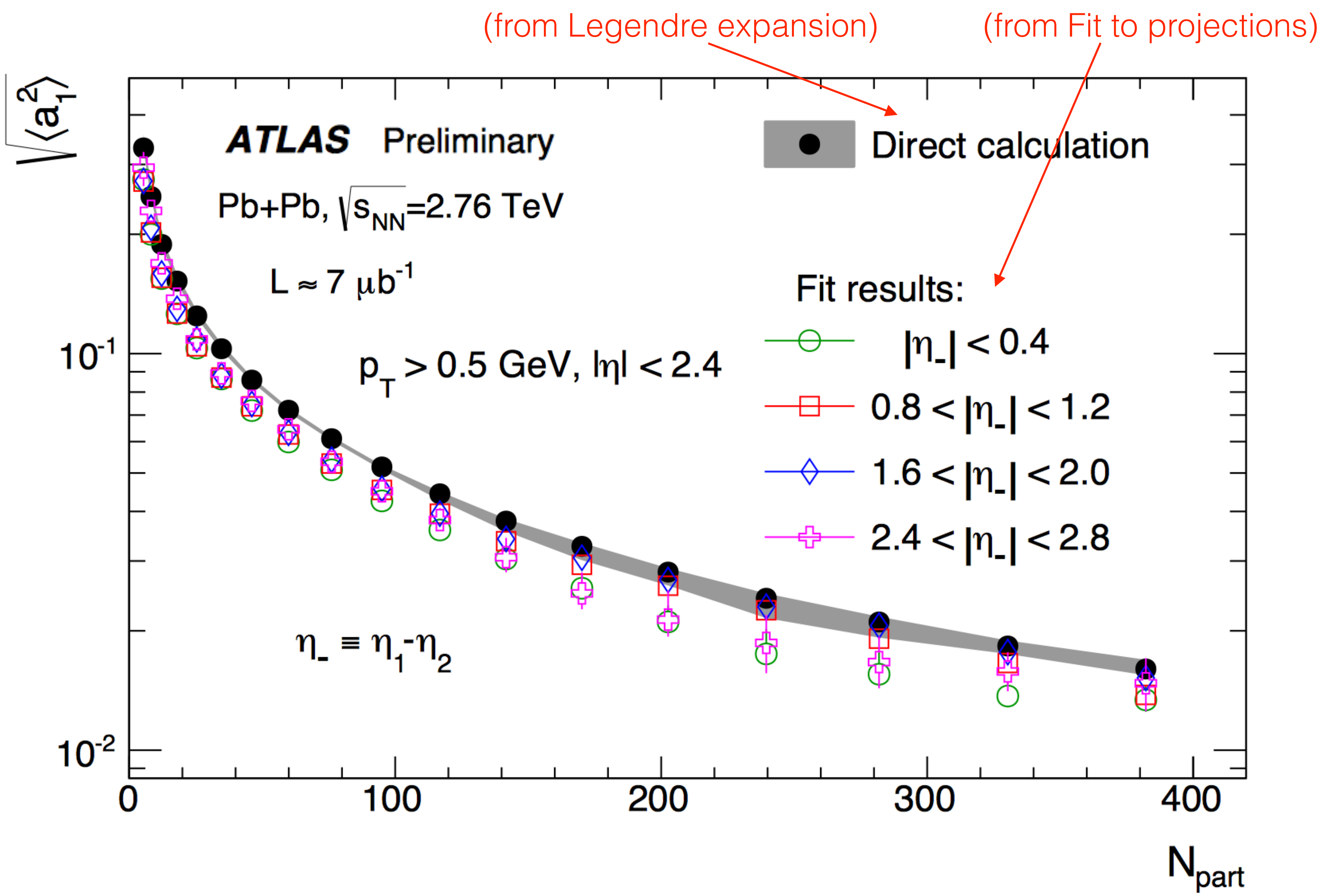

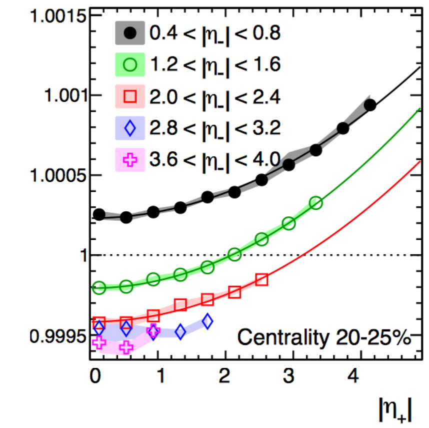

$C_N(\eta_+) = 0.065\langle a_1^2\rangle \eta_+^2 + b$

- Comparison of first order coefficient from Legendre expansion and from fit to projections.
- Similar centrality dependence, but values from fit always smaller than values from Legendre expansion.

Results: Comparison to Glauber model

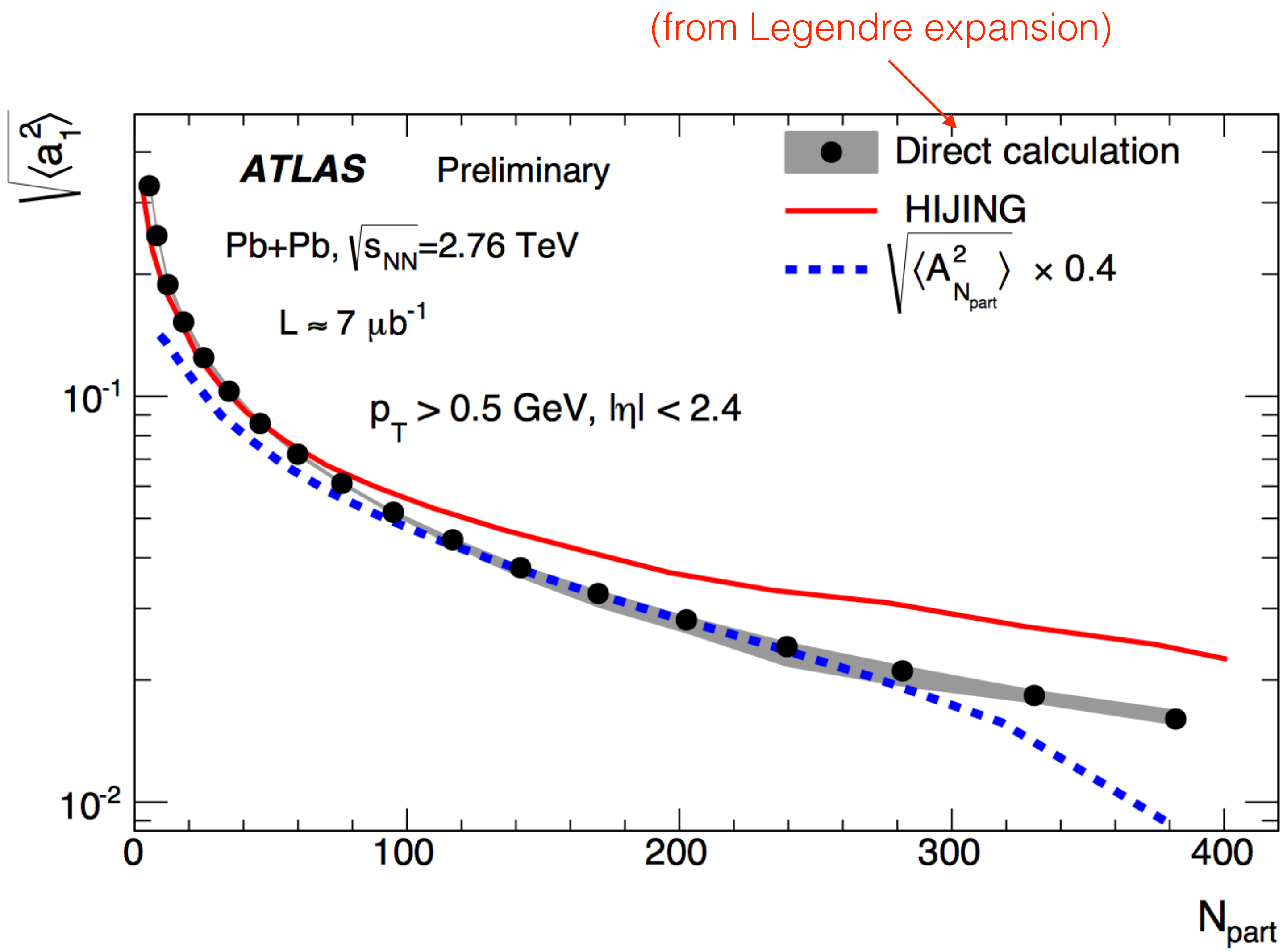

- Glauber model captures the centrality dependence of $\sqrt{\langle a_1^2 \rangle}$ in mid-central collisions.
- Fails in most central and peripheral classes, larger fluctuation than predicted by Glauber —> sub-nucleonic level fluctuations?

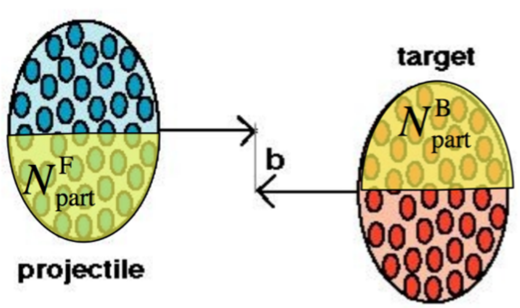

$$A_{N_{part}} = \frac{N^F_{part} - N^B_{part}}{N^F_{part} + N^B_{part}} .$$

Results: Comparison to HIJING

(from Legendre expansion)

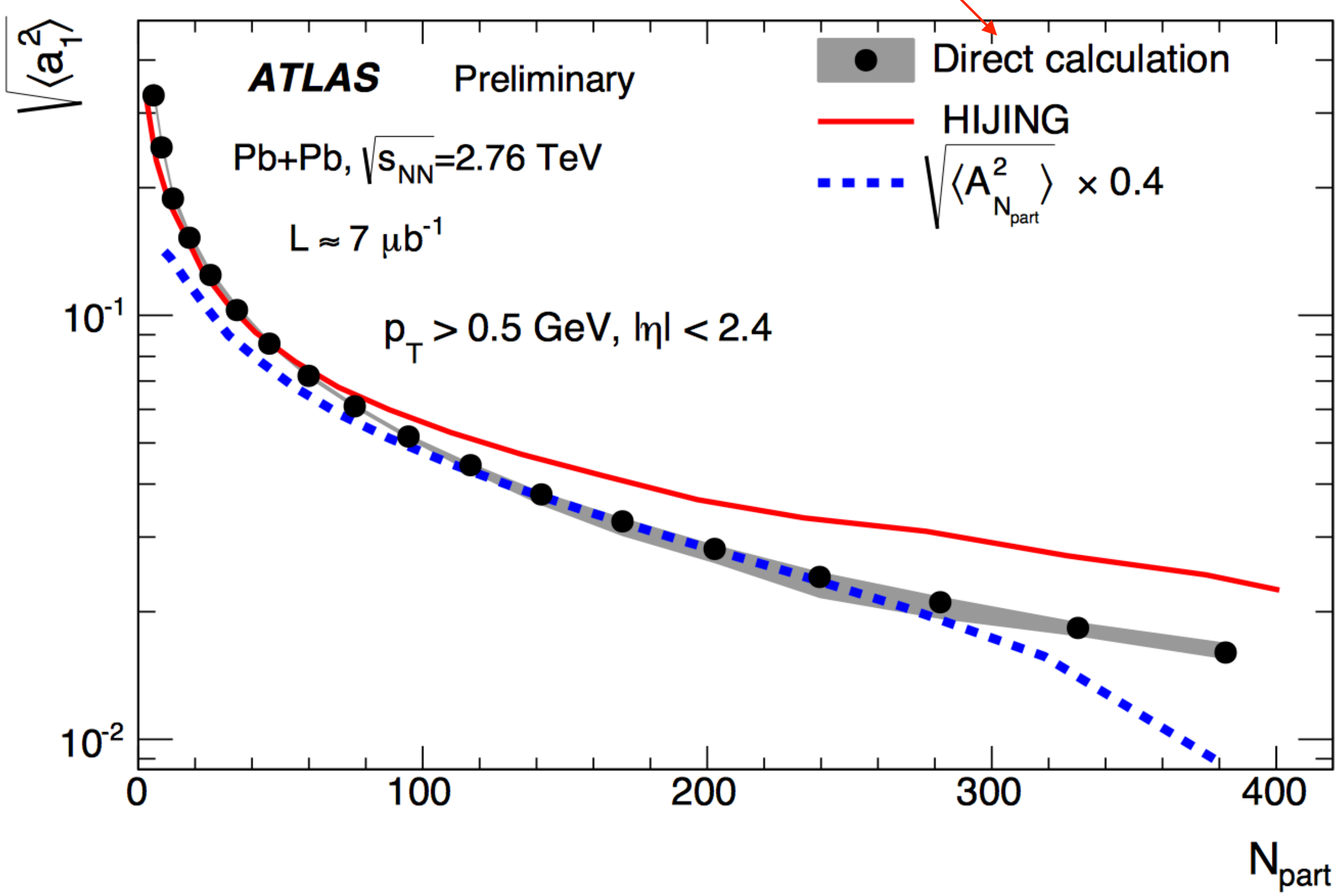

- Glauber model captures the centrality dependence of $\sqrt{\langle a_1^2 \rangle}$ in mid-central collisions.
- Fails in most central and peripheral classes, larger fluctuation than predicted by Glauber —> sub-nucleonic level fluctuations?
- Also shown are $\sqrt{\langle a_1^2 \rangle}$ from HIJING
- HIJING over-estimates $\sqrt{\langle a_1^2 \rangle}$ in mid-central and central collisions.

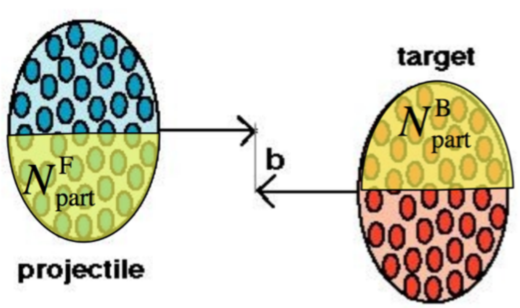

$$A_{N_{part}} = \frac{N^F_{part} - N^B_{part}}{N^F_{part} + N^B_{part}} .$$

Comparison to Model simulations

- Strong correlation of event-by-event a_1 with participant asymmetry is seen in models like HIJING

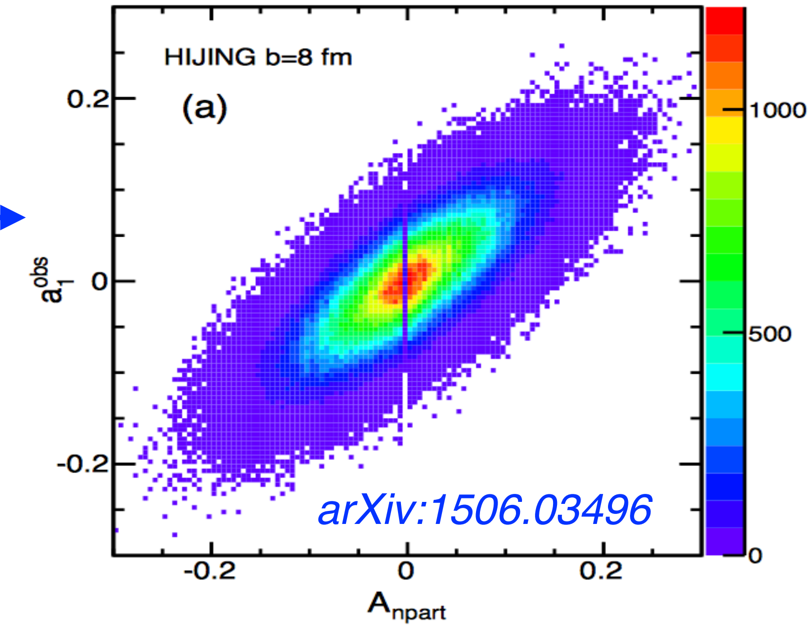

[see poster number A4-2 for more details]

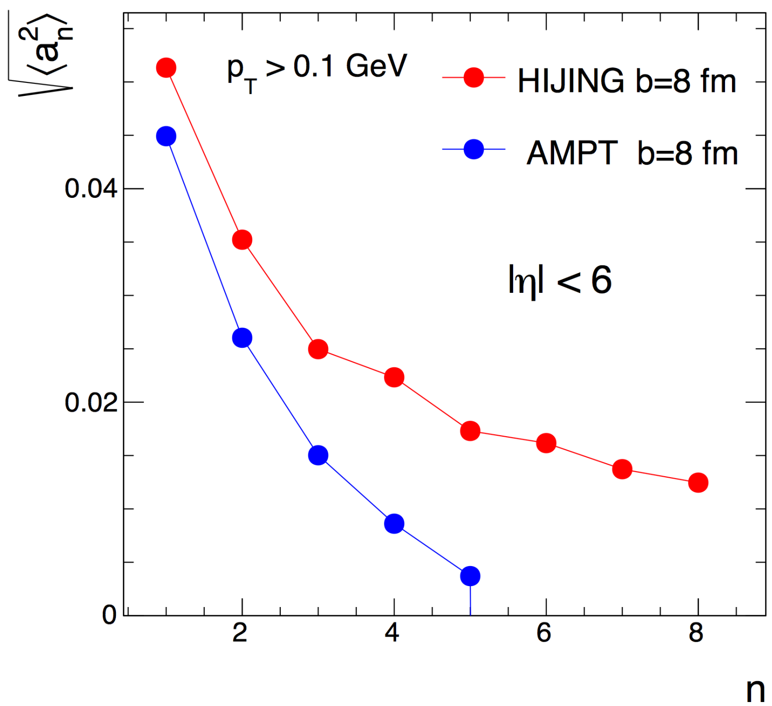

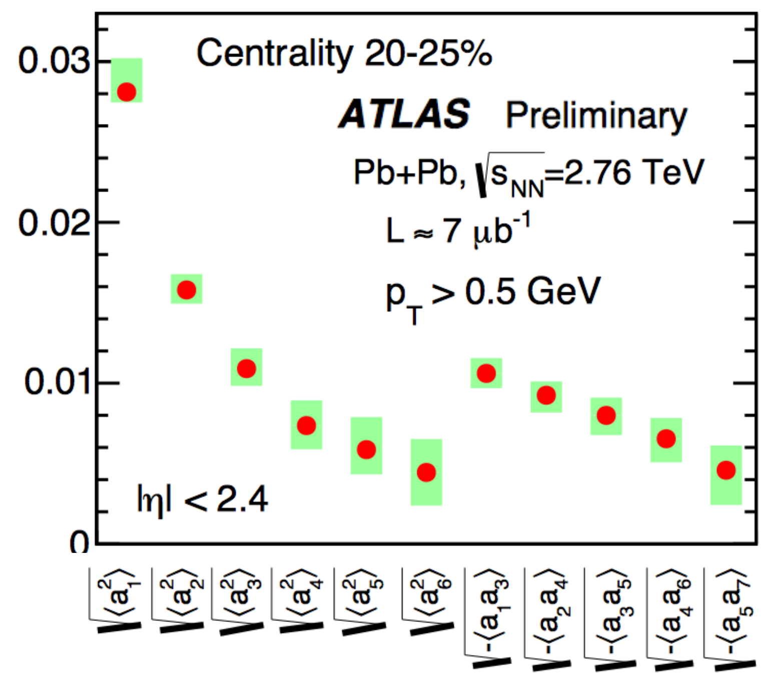

- $\sqrt{a_n^2}$ from HIJING larger than that from AMPT.
- HIJING shows slower decrease of $\sqrt{a_n^2}$ than data, AMPT shows slightly faster decrease.
- Effects of final state effects?

Summary and Conclusions

- Multiplicity correlations in longitudinal direction can provide information on the initial conditions in the longitudinal direction, and also final state correlations.

- Correlation functions:
  - Strength increases with centrality.
  - Dominated by quadratic rise along η_+ —> suggests that a_1 modulation is the largest.
  - Quadratic dependence is fit to obtain an estimate of $\sqrt{\langle a_1^2 \rangle}$.

- Legendre decomposition:
  - $\sqrt{\langle a_1^2 \rangle}$ modulation is the largest, magnitudes of higher orders decrease progressively.
  - Centrality dependence of $\sqrt{\langle A_{N_{part}}^2 \rangle}$ from Glauber model matches that of $\sqrt{\langle a_1^2 \rangle}$ in mid-central collisions, differences in central and peripheral collisions.
  - HIJING over-estimates $\sqrt{\langle a_n^2 \rangle}$ values.
  - Difference between HIJING, AMPT and data —> Medium effects?

- This and future measurements can provide important constraints on the initial conditions, particle production, medium evolution and final state correlations in the longitudinal direction

Back Up

Previous STAR and ALICE results

- Previous measurements focused on correlation coefficient between two symmetric rapidity windows.

$$b = \frac{\langle N_f N_b \rangle - \langle N_f \rangle \langle N_b \rangle}{\langle N_f^2 \rangle - \langle N_f \rangle^2}$$

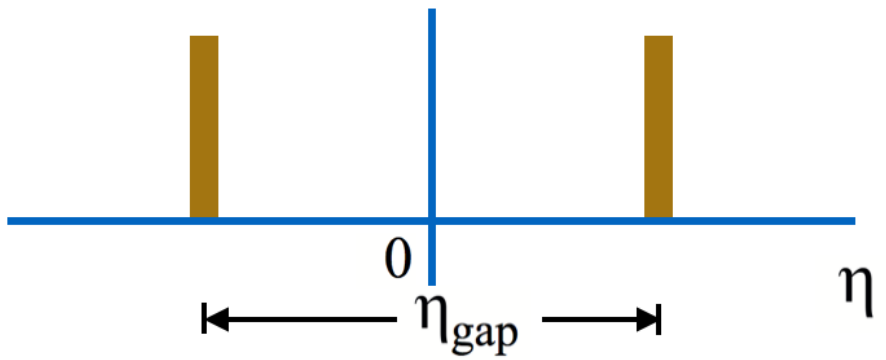

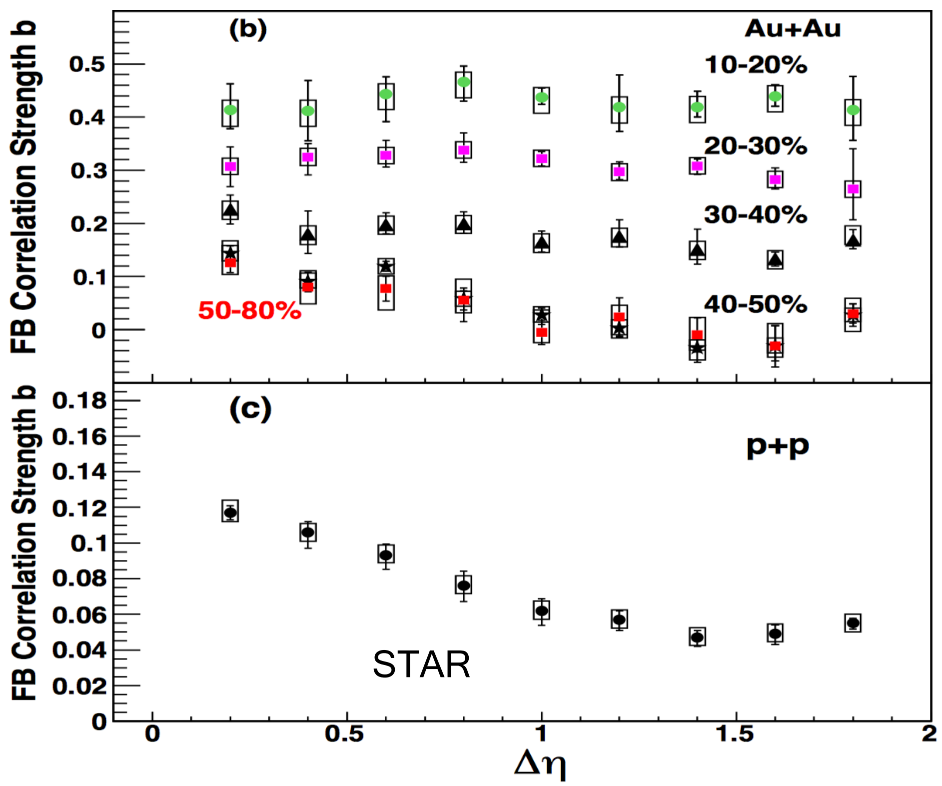

Phys.Rev.Lett. 103:172301,2009

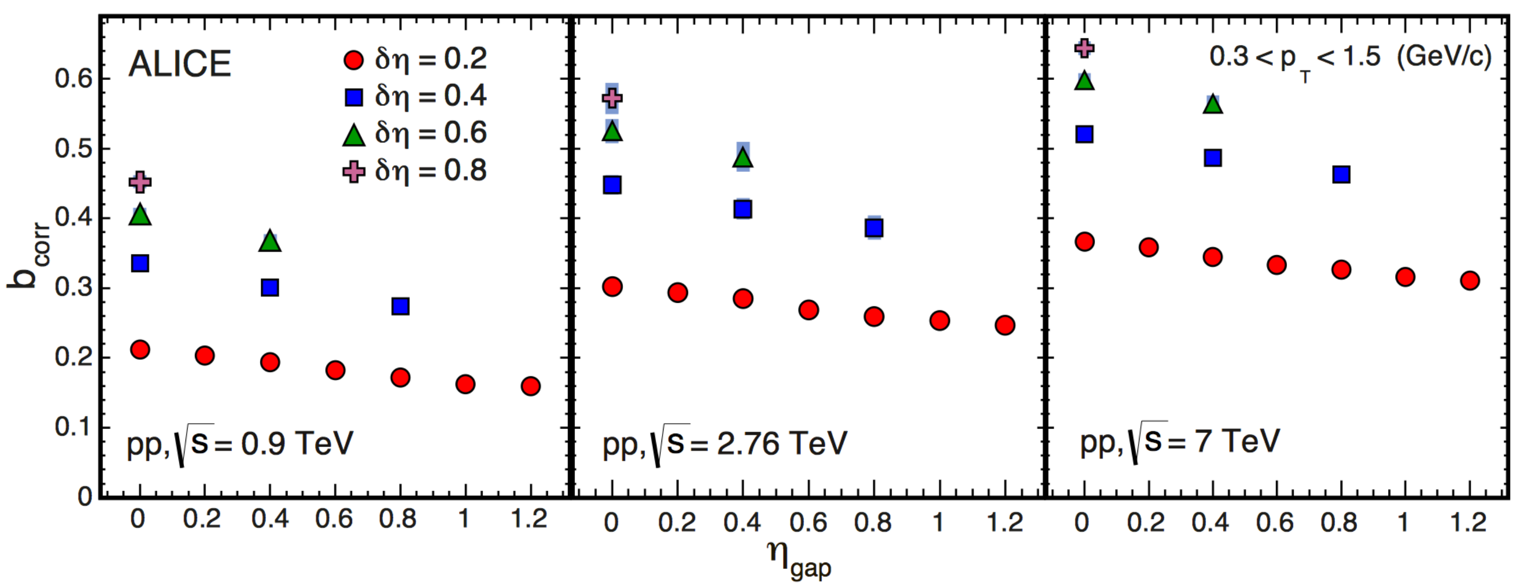

arXiv:1502.00230

Event-by-event modulations

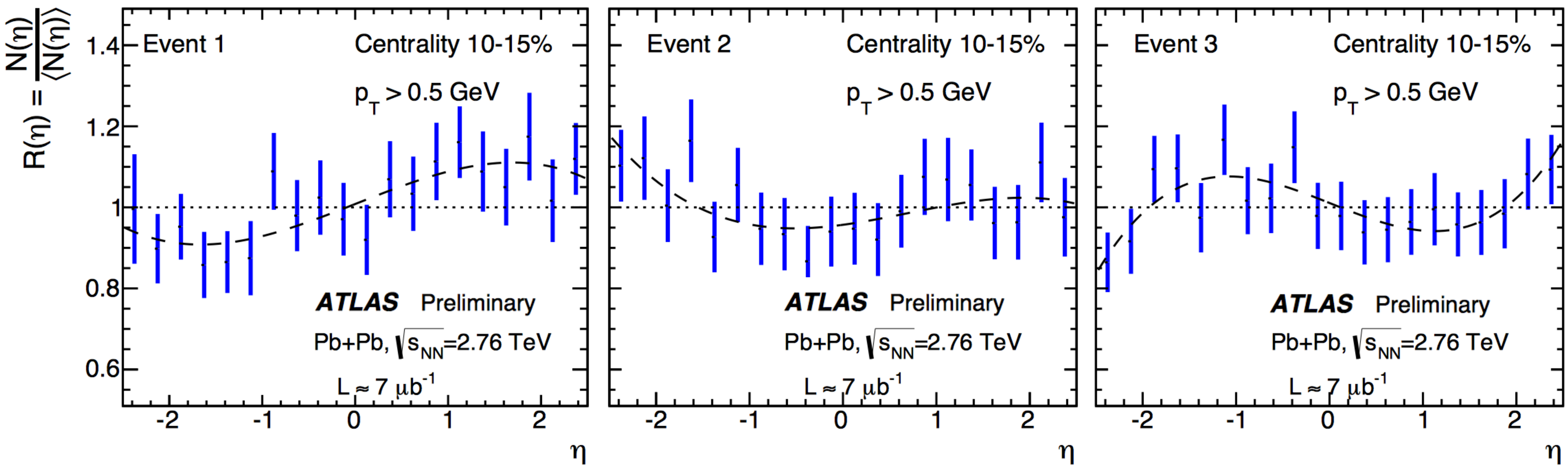

Statistical fluctuations

- Event by event modulations can also arise from statistical noise

$$N(\eta) = \langle N(\eta)\rangle \left(1 + \sum_{n=0}^{\infty} a_n T_n(\eta)\right), \quad T_n(\eta) = \sqrt{(}n + \frac{1}{2})P_n(\eta/Y)$$

- But these should average to zero in the CF, $C(\eta_1, \eta_2) = \dfrac{\langle N(\eta_1)N(\eta_2)\rangle}{\langle N(\eta_1)\rangle\langle N(\eta_2)\rangle}$

- since
  - a) Statistical fluctuations in two different η are uncorrelated
  - b) Self correlations are not counted in the CF
    when $\eta_1 = \eta_2$, statistical fluctuations dont average to zero and equals $\langle N(\eta)\rangle$
    which is same as the number of self-correlations.

- So the $\langle a_n a_m\rangle$ from CFs are quantities unfolded for statistical noise.

Analysis procedure: Residual centrality dependence

$$N(\eta) = \langle N(\eta) \rangle \left(1 + \sum_{n=0}^{\infty} a_n T_n(\eta) \right)$$

$$C(\eta_1, \eta_2) = \frac{\langle N(\eta_1) N(\eta_2) \rangle}{\langle N(\eta_1) \rangle \langle N(\eta_2) \rangle}$$

- Multiplicity width of bins used for normalizing affect CFs

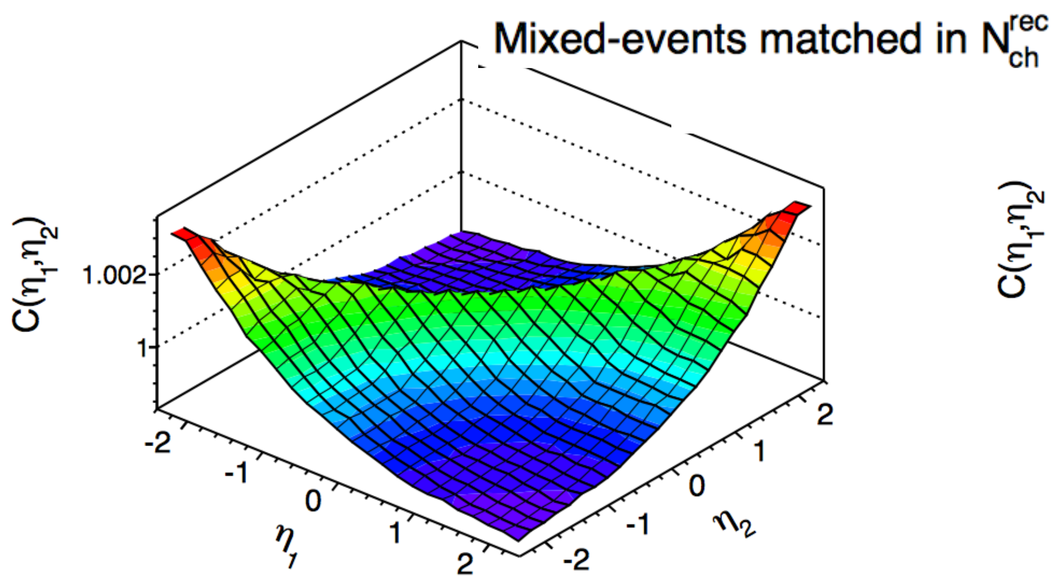

narrow range in multiplicity

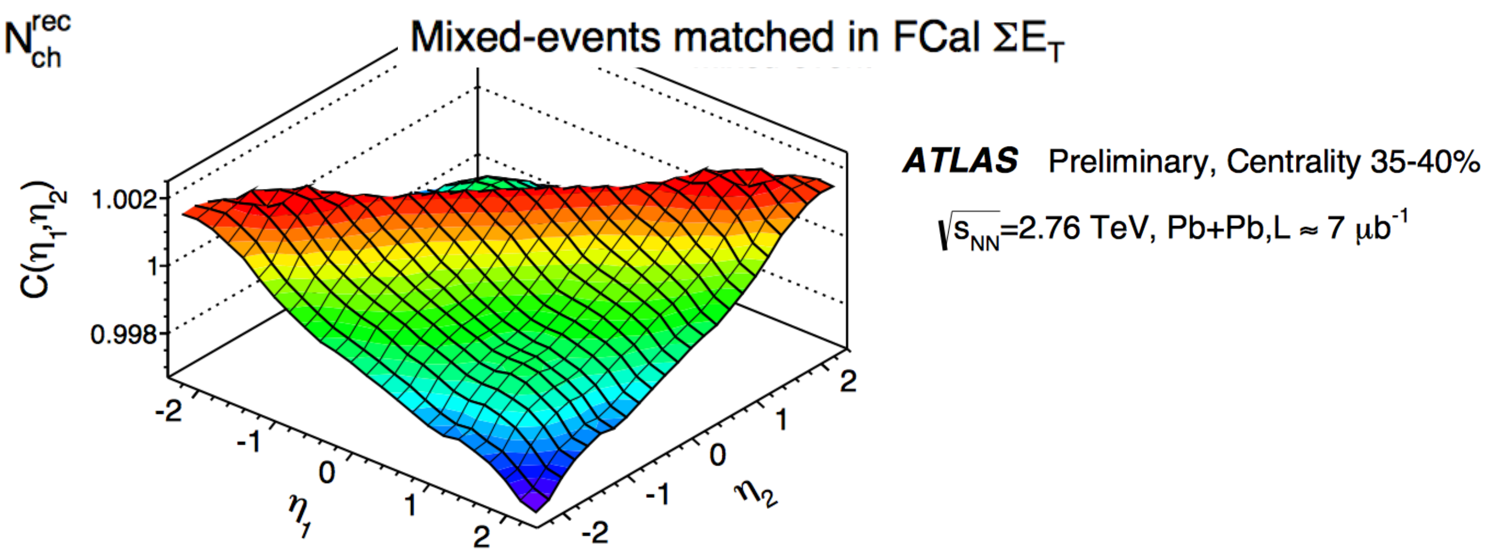

broader range in multiplicity

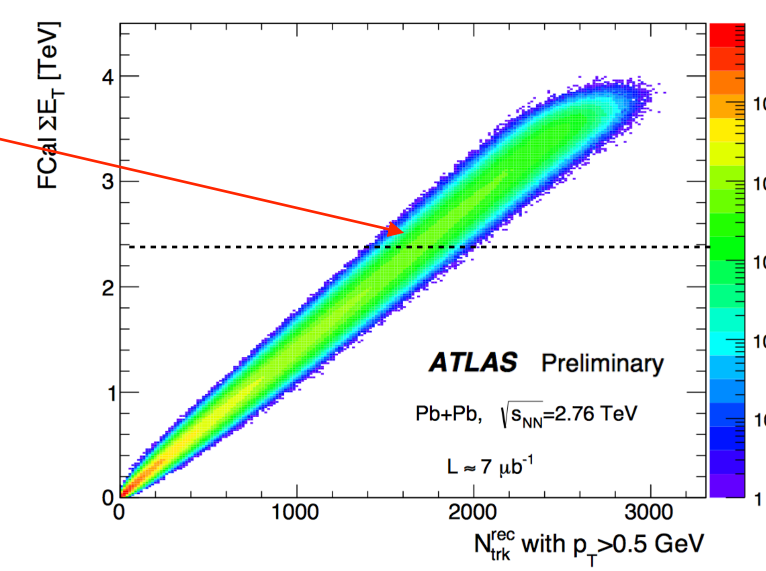

Analysis procedure: Residual centrality dependence

$$C(\eta_1, \eta_2) = \frac{\langle N(\eta_1) N(\eta_2) \rangle}{\langle N(\eta_1) \rangle \langle N(\eta_2) \rangle}$$

- Multiplicity width of bins used for normalizing affect CFs

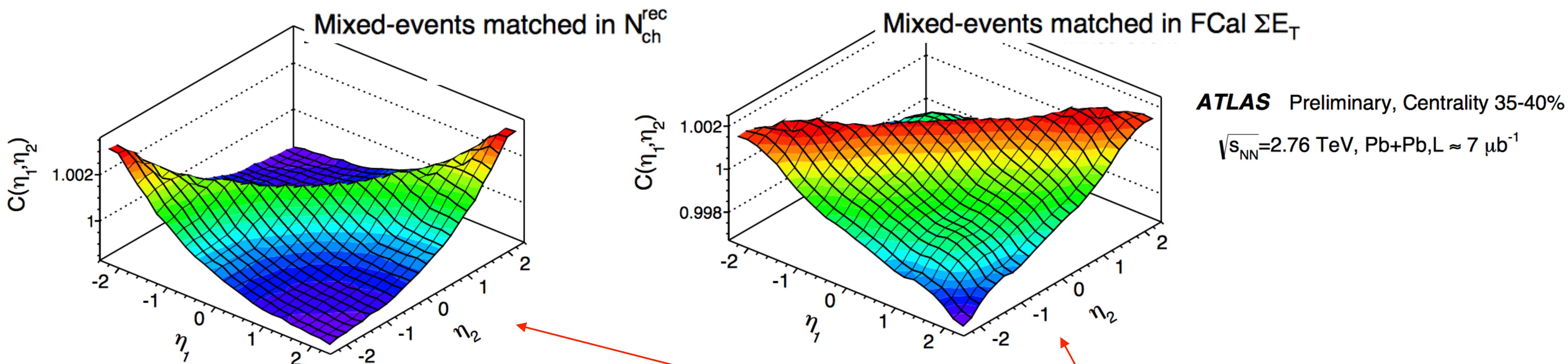

Change of shape with multiplicity causes CFs to look different

- But can be easily decoupled

$$C(\eta_1, \eta_2) = 1 + \langle a_0 a_0 \rangle + \sum_{n=1}^{\infty} \langle a_0 a_n \rangle \left(T_n(\eta_2) + T_n(\eta_1)\right) + \sum_{n,m=1}^{\infty} \langle a_n a_m \rangle \frac{\left(T_n(\eta_1) T_m(\eta_2) + T_n(\eta_2) T_m(\eta_1)\right)}{2}$$

overall multiplicity fluctuations

change of shape with multiplicity

intrinsic shape fluctuations at a given multiplicity

Analysis procedure: Residual centrality dependence

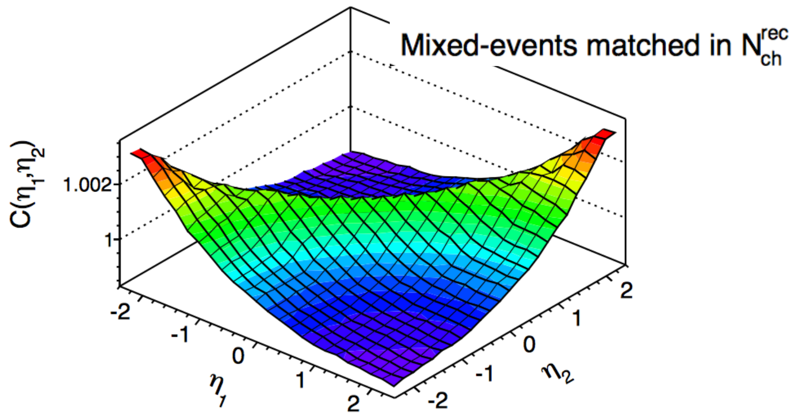

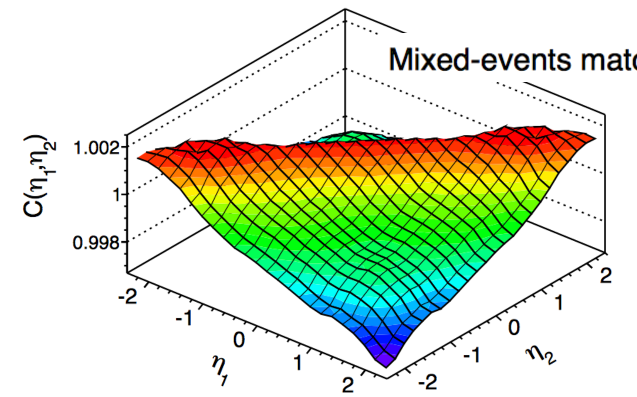

ATLAS Preliminary, Centrality 35-40%

$\sqrt{s_{NN}}$=2.76 TeV, Pb+Pb,L ≈ 7 μb^{-1}

$$C(\eta_1,\eta_2) = 1 + \langle a_0 a_0\rangle + \sum_{n=1}^{\infty}\langle a_0 a_n\rangle\left(T_n(\eta_2)+T_n(\eta_1)\right) + \sum_{n,m=1}^{\infty}\langle a_n a_m\rangle\frac{\left(T_n(\eta_1)T_m(\eta_2)+T_n(\eta_2)T_m(\eta_1)\right)}{2}$$

- Can be removed by rescaling with the projections

$$C_N(\eta_1,\eta_2) = \frac{C(\eta_1,\eta_2)}{C_p(\eta_1)C_p(\eta_2)} \qquad C_p(\eta_1) = \int\frac{C(\eta_1,\eta_2)}{2Y}d\eta_2, C_p(\eta_2) = \int\frac{C(\eta_1,\eta_2)}{2Y}d\eta_1; Y=2.4$$

ATLAS Preliminary, Centrality 35-40%

$\sqrt{s_{NN}}$=2.76 TeV, Pb+Pb,L ≈ 7 μb^{-1}

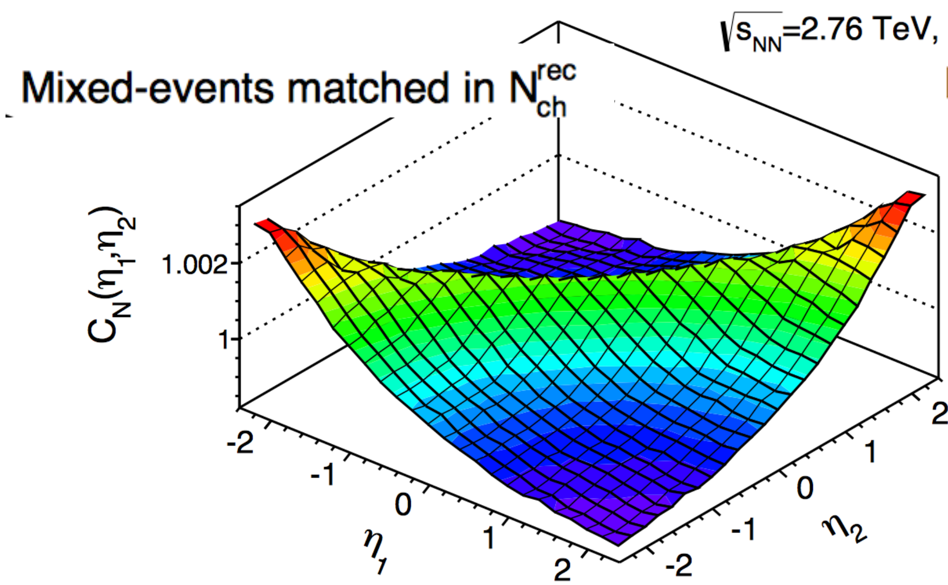

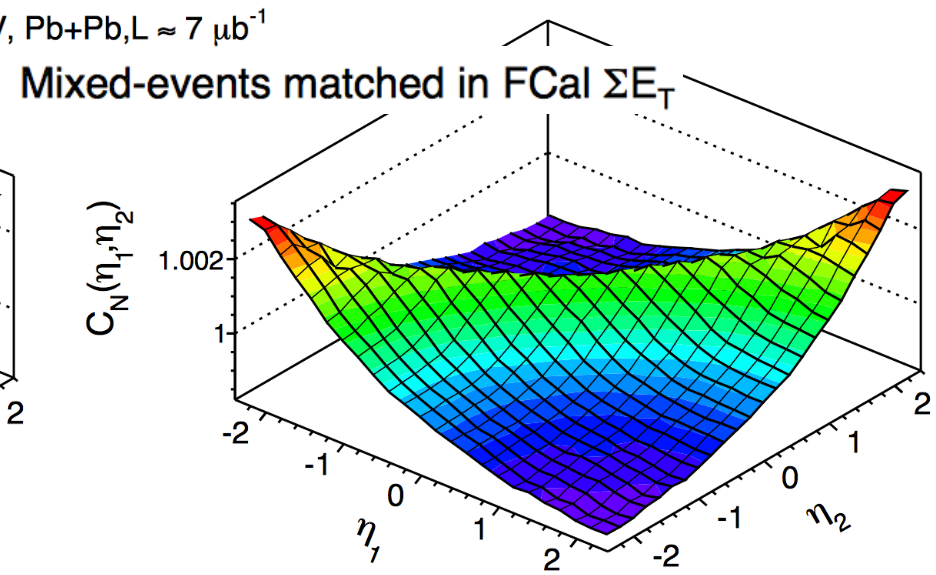

After rescaling by projections correlation functions are consistent irrespective of mixing bin widths

Analysis procedure: Residual centrality dependence

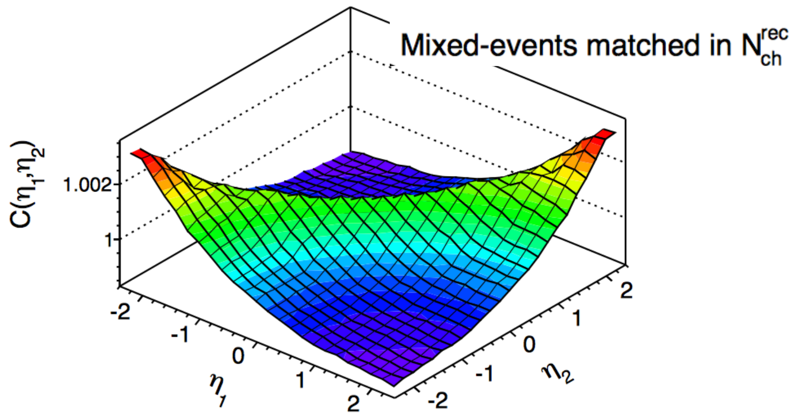

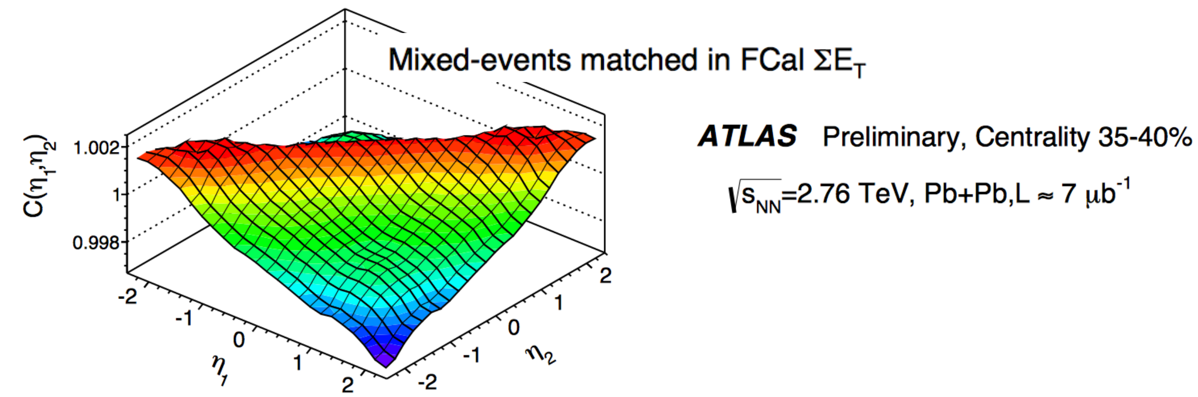

$$C(\eta_1,\eta_2) = 1 + \langle a_0 a_0 \rangle + \sum_{n=1}^{\infty} \langle a_0 a_n \rangle \left(T_n(\eta_2) + T_n(\eta_1) \right) + \sum_{n,m=1}^{\infty} \langle a_n a_m \rangle \frac{(T_n(\eta_1)T_m(\eta_2) + T_n(\eta_2)T_m(\eta_1))}{2}$$

- Can be removed by rescaling with the projections

$$C_N(\eta_1,\eta_2) = \frac{C(\eta_1,\eta_2)}{C_p(\eta_1)C_p(\eta_2)} \qquad C_p(\eta_1) = \int \frac{C(\eta_1,\eta_2)}{2Y} d\eta_2, C_p(\eta_2) = \int \frac{C(\eta_1,\eta_2)}{2Y} d\eta_1; Y = 2.4$$

$$C_N(\eta_1,\eta_2) = 1 + \sum_{n=1}^{\infty} \langle a_n a_m \rangle \left(\frac{T_n(\eta_1)T_m(\eta_2) + T_n(\eta_2)T_m(\eta_1)}{2} \right)$$

- Shape fluctuations at a given multiplicity are captured by $\langle a_n a_m \rangle$ with n,m >= 1.

see arXiv:1506.03496 for more details

Projections - II

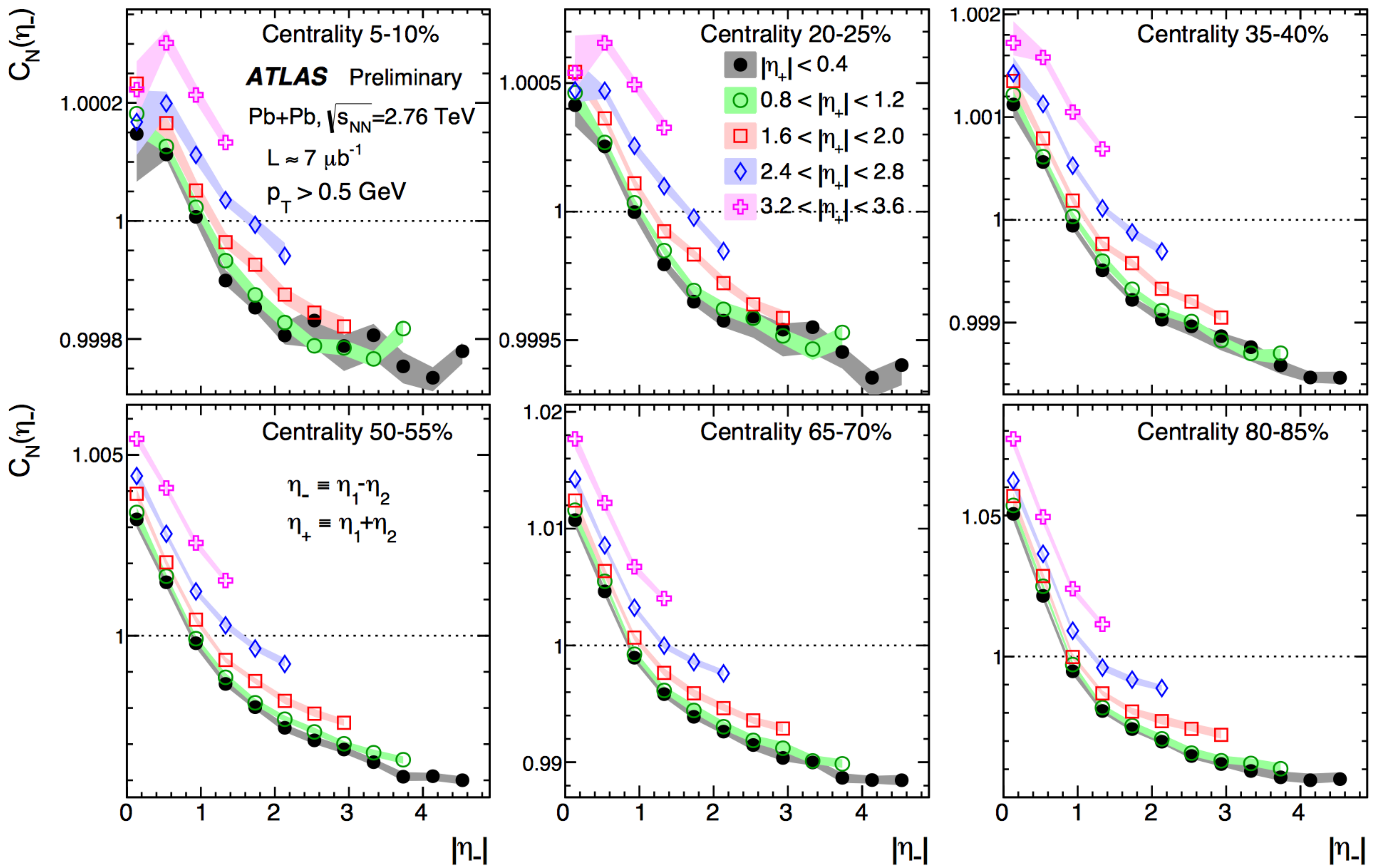

Projections - III

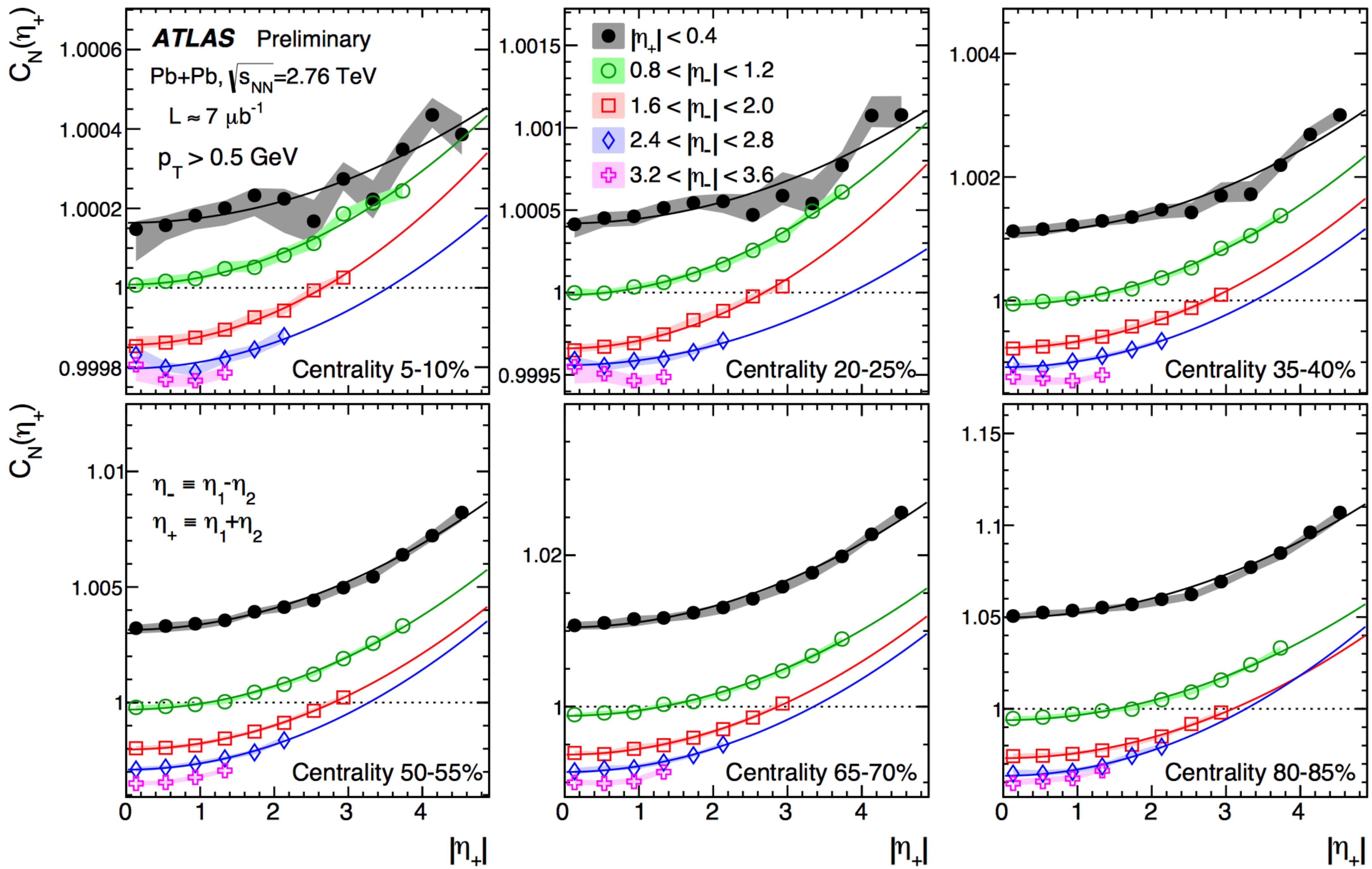

Comparison with HIJING - II

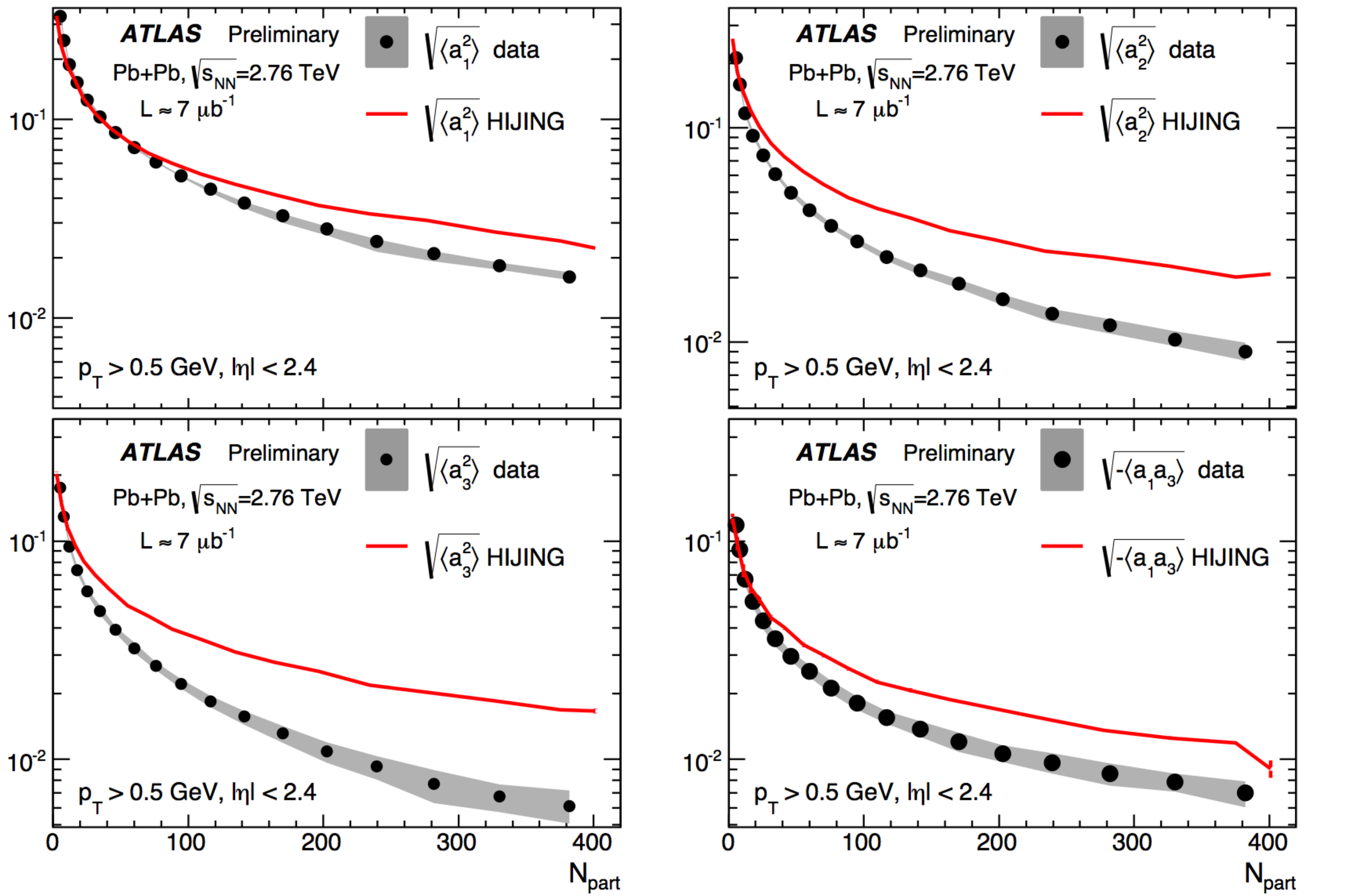

Spectra - II

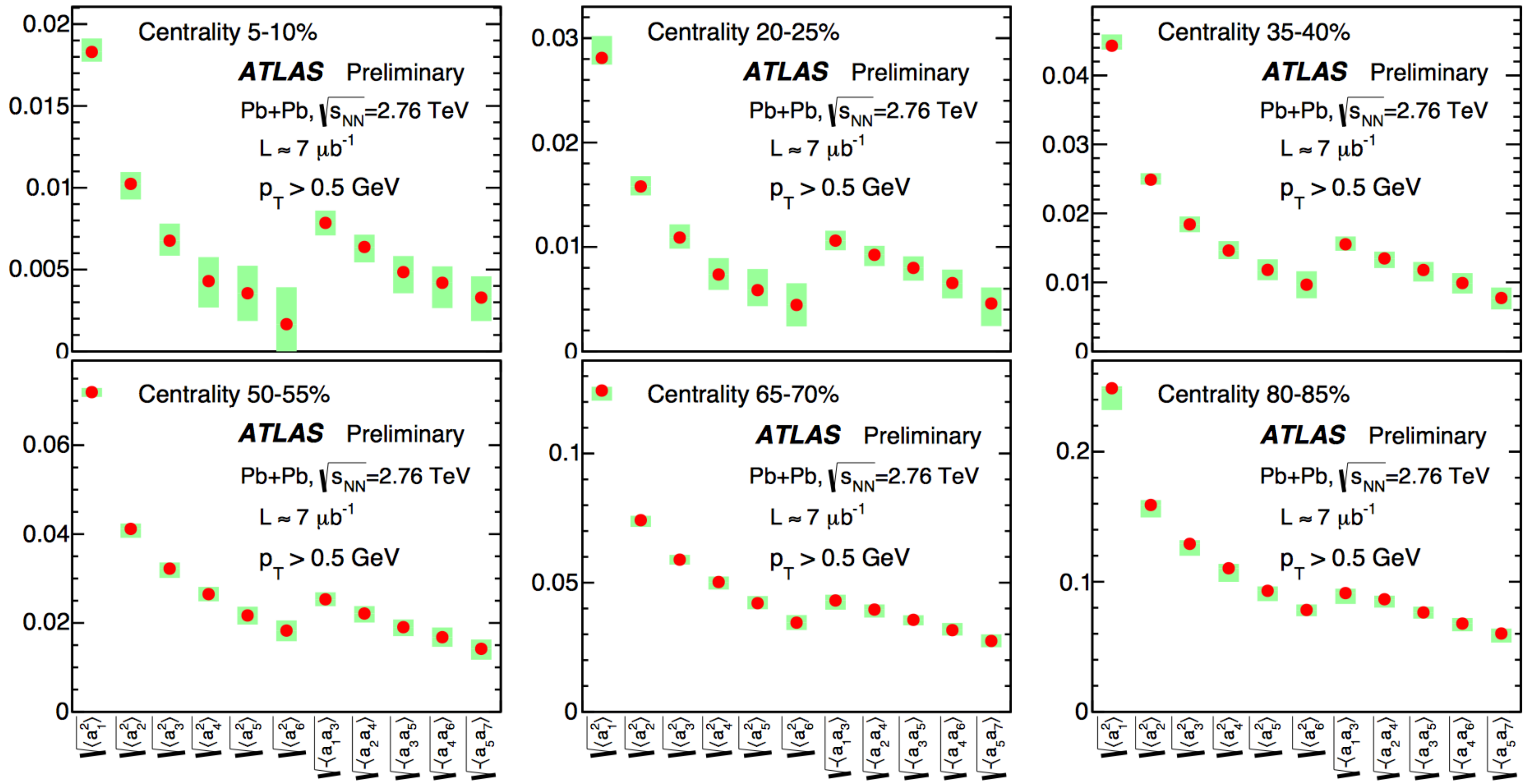
Centrality 5-10%
Centrality 20-25%
Centrality 35-40%
Centrality 50-55%
Centrality 65-70%
Centrality 80-85%
ATLAS Preliminary
Pb+Pb, $\sqrt{s_{NN}}$=2.76 TeV
L ≈ 7 μb^{-1}
p_T > 0.5 GeV
$\langle a_1^2\rangle$ $\langle a_2^2\rangle$ $\langle a_3^2\rangle$ $\langle a_4^2\rangle$ $\langle a_5^2\rangle$ $\langle a_6^2\rangle$ $\langle a_1a_3\rangle$ $\langle a_2a_4\rangle$ $\langle a_3a_5\rangle$ $\langle a_4a_6\rangle$ $\langle a_5a_7\rangle$

Ridge in p+Pb collisions

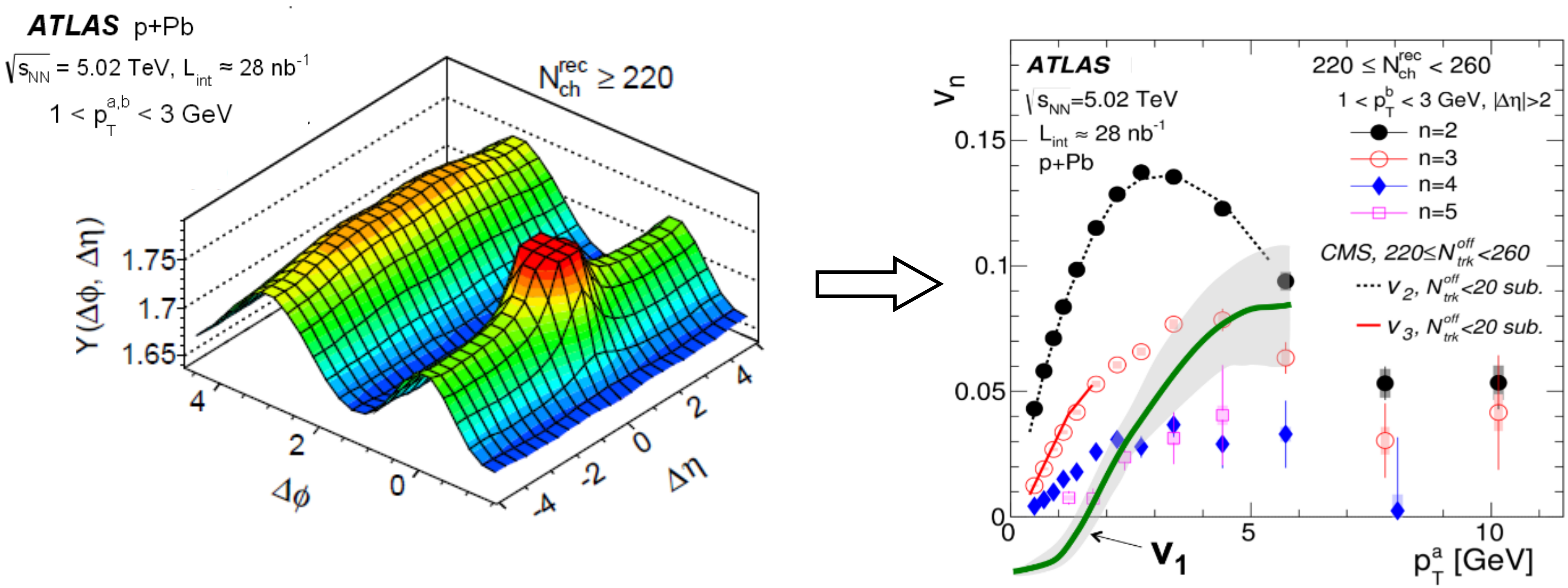

- Long-range azimuthal correlations in high multiplicity p+Pb collisions.
- Fourier harmonics $v_1 - v_5$ extracted from the two-particle correlations.
- Recoil subtraction is applied to remove contribution from away-side jets, resonances etc.

- v_n show similar shape in p_T as those in A-A collisions.
- Decrease with increasing n
- Large v_1 that changes sign with p_T also observed.

Recoil subtraction

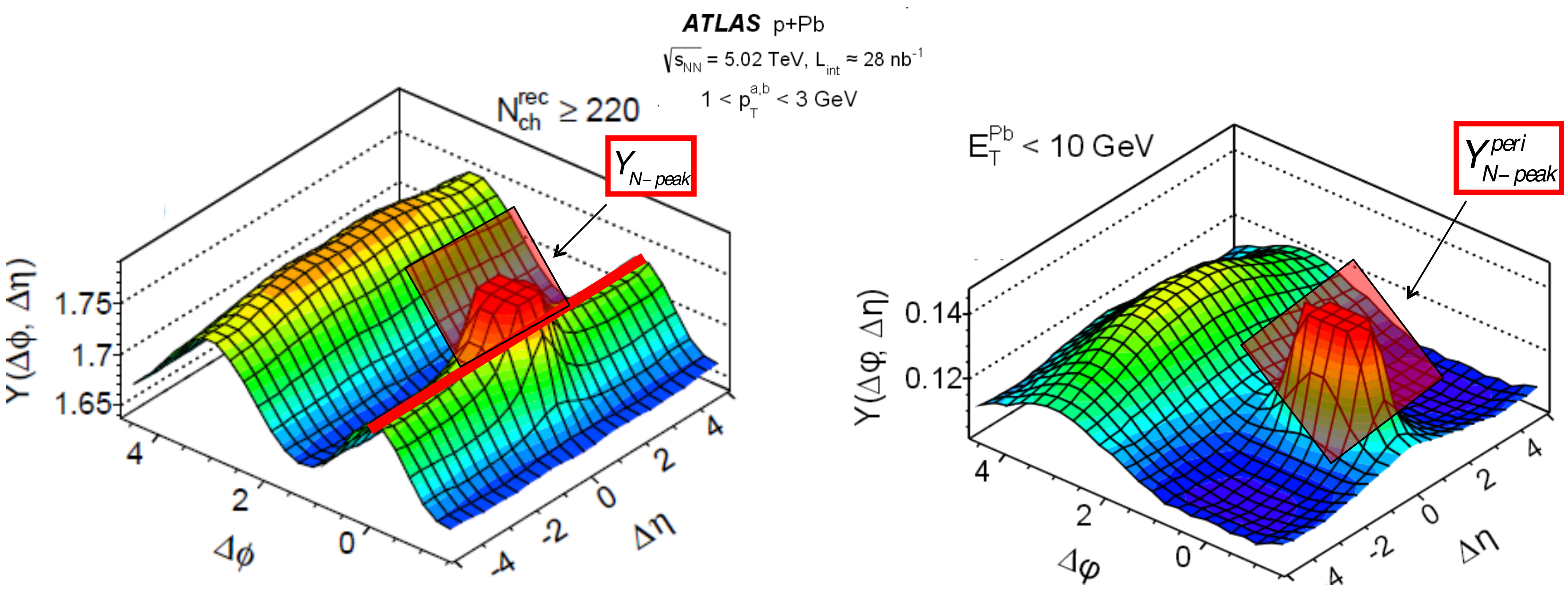

$$Y^{sub}(\Delta\phi,\Delta\eta) = Y(\Delta\phi,\Delta\eta) - \alpha Y^{corr}_{peri}(\Delta\phi,\Delta\eta)$$

- α is chosen such that $\alpha Y^{peri}_{N-peak} = Y_{N-peak}$
- Peripheral bin is taken to be one with total FCal energy, E_T^{Pb} < 10 GeV

$$Y^{\text{N-Peak}} = \int_{|\Delta\eta|<1} Y(\Delta\eta)d\Delta\eta - \frac{1}{3}\int_{2<|\Delta\eta|<5} Y(\Delta\eta)d\Delta\eta$$

$$Y^{\text{corr}}(\Delta\phi,\Delta\eta) = \frac{\int B(\Delta\phi,\Delta\eta)d\Delta\phi d\Delta\eta}{\pi\eta_\Delta^{\text{max}}}\left(\frac{S(\Delta\phi,\Delta\eta)}{B(\Delta\phi,\Delta\eta)} - b_{\text{ZYAM}}\right)$$

Dipolar flow

- In A+A collisions a rapidity even first order flow (v_1) is observed.

Phys.Rev. C86 (2012) 014907

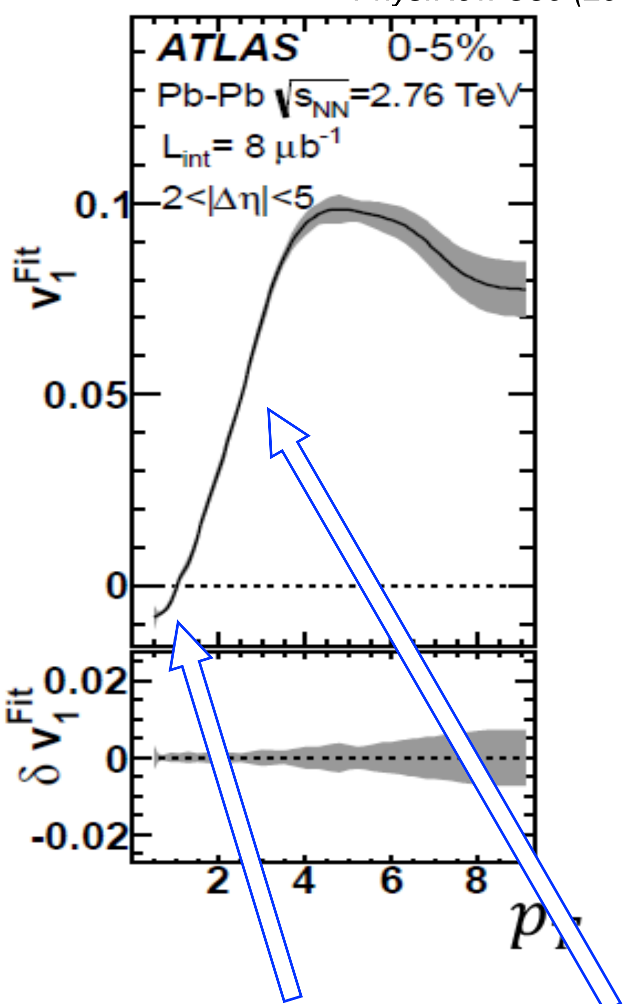

-ve at low p_T, +ve at higher p_T

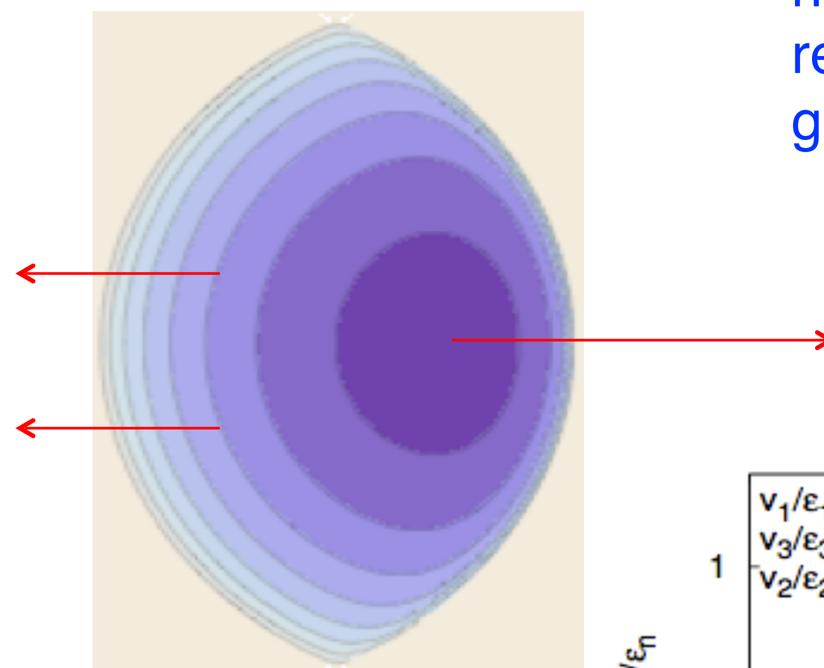

- Arises from hydrodynamic response to initial geometry

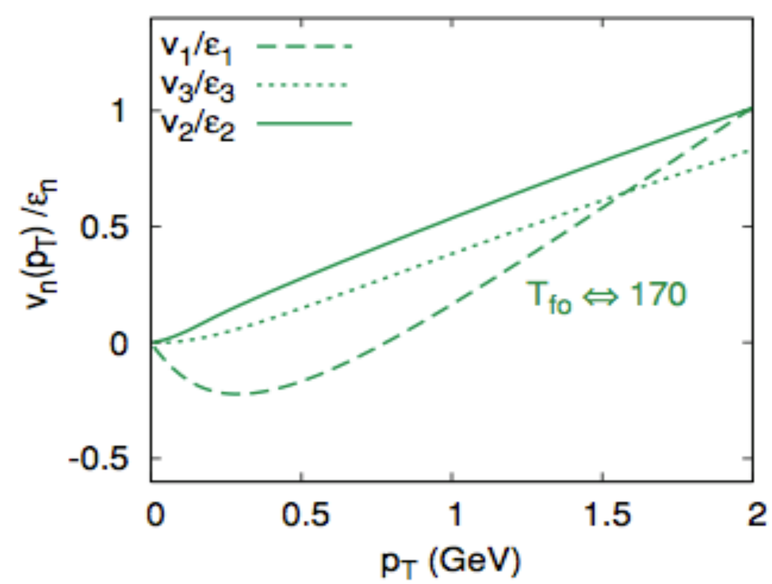

Dipolar flow

- In A+A collisions a rapidity even first order flow (v_1) is observed.
- Arises from hydrodynamic response to initial geometry

Phys.Rev. C86 (2012,

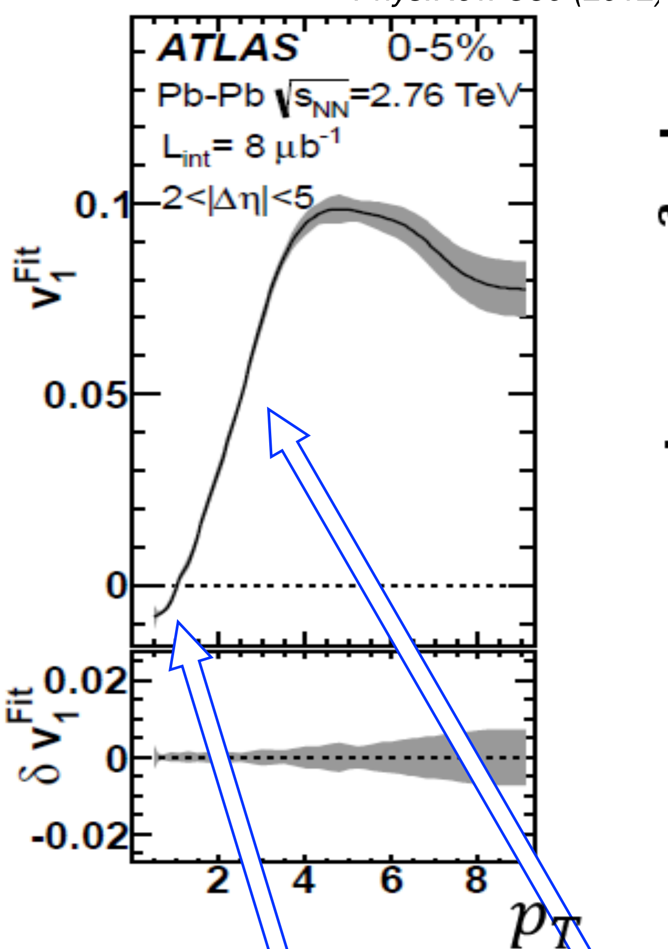

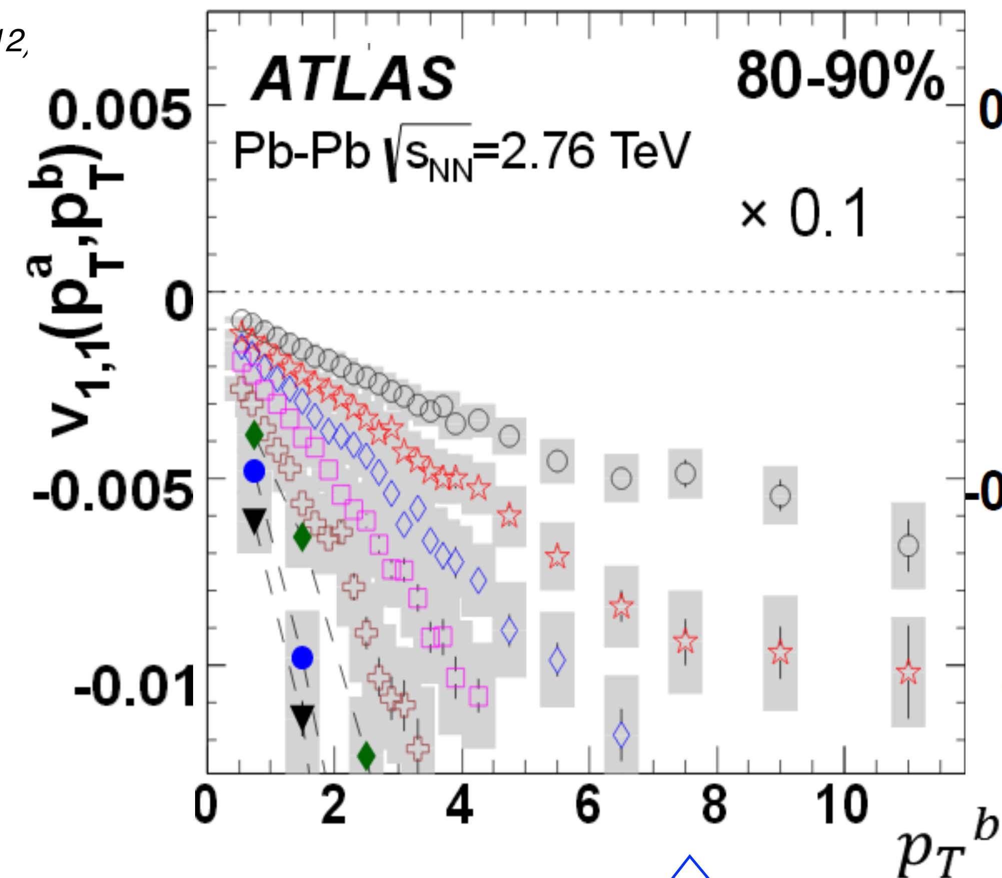

Phys.Rev. C86 (2012) 014907

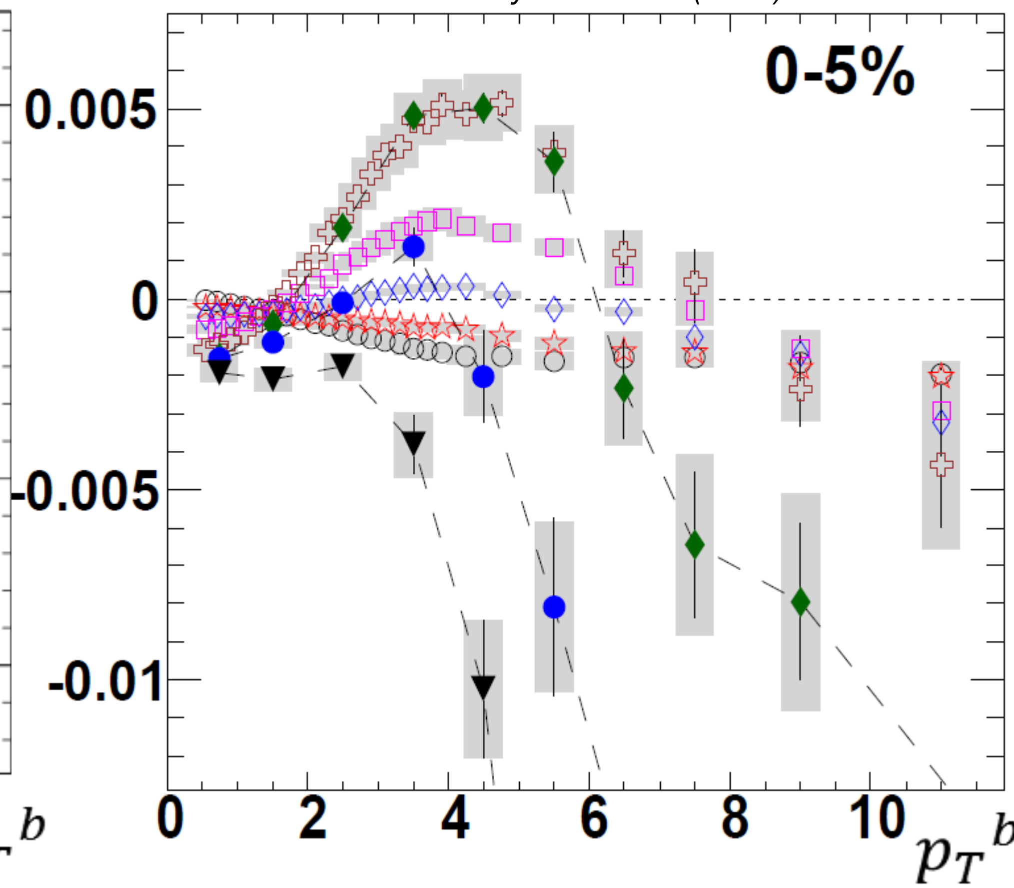

-ve at low p_T, +ve at higher p_T

Mom. conservation

Mom. Conservation + flow

- Also has a momentum conservation component at 2PC

$$v_{1,1}\left(p_T^a, p_T^b\right) = v_1(p_T^a)v_1(p_T^b) - Kp_T^a p_T^b$$

Dipolar flow in p+Pb

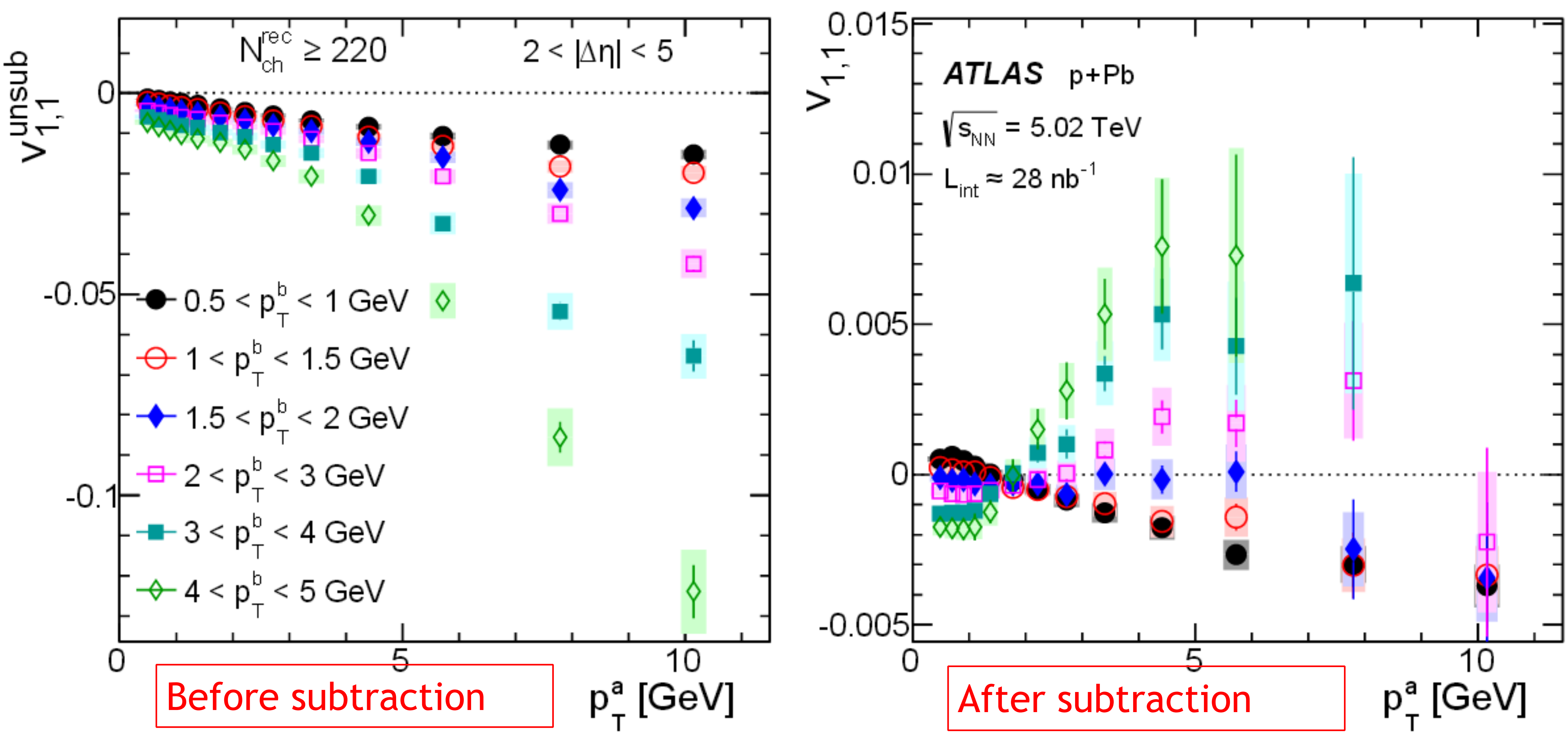

- Before recoil subtraction, the first order harmonic reflect mostly the momentum conservation effect
- After recoil subtraction show characteristic p_T dependence of dipolar flow
  - Similar to that seen in central Pb+Pb collisions

v_n scaling between the p+Pb and Pb+Pb systems

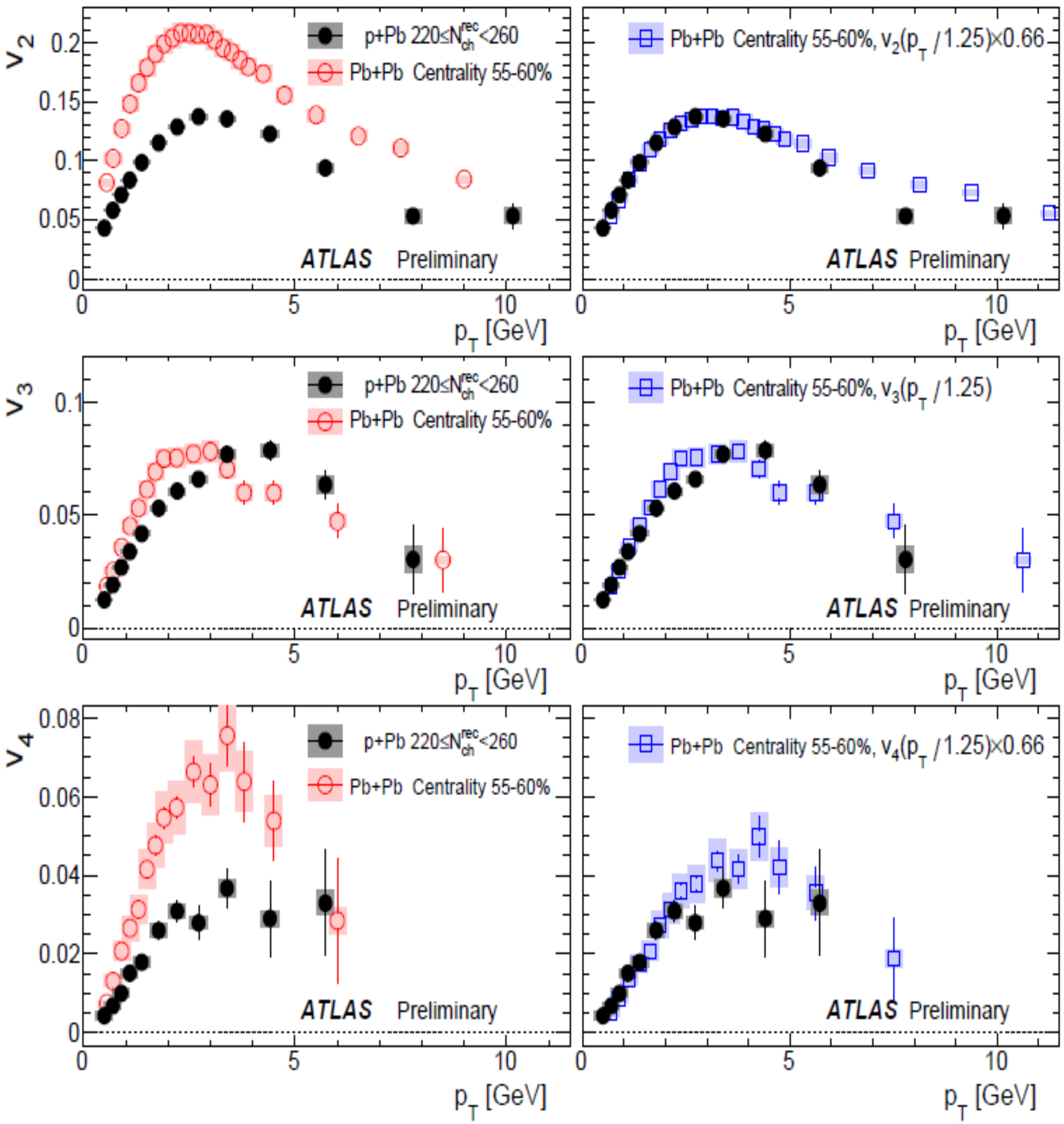

- Consistent v_3 values between the two systems at similar multiplicity
- v_2 values, after scaling the p_T axis differ only by a scale factor between the two systems.
- Suggests a similar origin for v_n in the two systems and similar medium response to initial geometry.